LHC Project Note 341

3/23/04

Adriana.Rossi@cern.ch

VASCO (VAcuum Stability COde): multi-gas code to calculate gas density profile in a UHV system

A. Rossi / AT-VAC

Keywords: vacuum calculations, vacuum stability, residual gas pressure, induced desorption

Summary

Calculation of the residual gas pressure in the presence of hadron beam.

1. Introduction

In a particle accelerator the estimation of residual gas density profiles is indispensable to verify the design and confirm vacuum stability [1] and beam lifetime. Moreover, in the experimental insertion regions density profiles are extremely important to estimate machine background effects in the detectors generated by proton or ion-gas scattering.

In a hadron collider, beam induced dynamic effects such as ion, electron and photon-stimulated gas desorption are the main source of residual gas.

In this paper, the VASCO code to estimate vacuum stability and density profiles in steady state conditions is presented. In order to take into account the variation of geometry of the vacuum system, surface materials, temperature, surface treatment and conditioning along the accelerator ring, the code treats the vacuum system as a sequence of elements linked with boundary conditions. The nomenclature and symbols refer to the Large Hadron Collider geometry, but can be applied to any vacuum system.

The model and assumptions used in VASCO are described in section 2. The equations inferred from the model are detailed in sections 3 and 4. The mathematical implementation and boundary conditions are specified in sections 5 and 6. Section 7 gives the final equations to be solved.

2. Vacuum model

In the model used for vacuum calculations [2], it is assumed that the rate of change of number of molecules per unit volume (schematically shown in Figure 1 and described in the equations below) depends on:

- Molecular diffusion along the chamber due to pressure gradient;
- Beam induced dynamic effects such as ion, electron and photon-stimulated gas desorption;
- Gas pumping distributed along the pipe: in the case of the LHC Non Evaporable Getter coatings in the room temperature sections; Cryo-pumping or pumping through beam screen holes in the magnets working at cryogenic temperature; Beam induced pumping as explained in following sections;
- Gas lumped pumping (provided by Sputtered Ion pumps in the LHC).

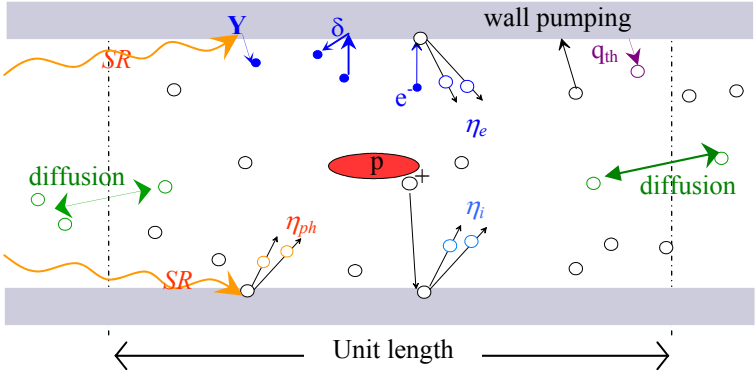

Figure 1

The model used in the VASCO code utilises:

- **Cylindrical geometry**: This allows for one-dimensional approximation (along the beam axis), assuming radial symmetry. Chambers with non-cylindrical cross sections (i.e. conical or elliptical) are approximated with cylinders having the same conductance. When a parameter is a function of the wall surface area (for ex. thermal outgassing and wall pumping) it is scaled to take the real area into account.
- **Time invariant parameters**: This implies that the residual gas density estimation is relevant to a specific moment in time, since some of the parameter are indirectly time dependent such as: a) Induced gas desorption yields (η) and photoelectron yield (Y), which depend on the surface history (wall pre-conditioning, particle bombardment) and, on the cryogenic surfaces, change with the amount of gas condensed on the surface; b) NEG distributed pumping which varies with the quantity of gas already pumped and the activation history.
- **Multi-gas model**: The model takes into account the cross-desorption by ions of one gas species of other adsorbed gas species. This implies that the equation for one gas species density is linked to other gas species density.
- **Finite elements**: Each element is characterised by a different set of parameters (for example a different cross section dimension, material properties, lumped pumping at the extremities, etc.). The boundary conditions are set to ensure the continuity of the gas density and flux functions between elements. For the first and the last elements, where there are no lumped pumps, "mirror" boundary conditions are adopted. In other words it is supposed that the sector considered is closed on both sides, and molecules travelling in the outward direction are reflected back into the system. If there are lumped pumps, the pumping speed is halved assuming that the extremity is open and the adjacent pipe has the same cross section.

3. Equations governing the dynamic density evolution in a vacuum system: single-gas model

In the 'single-gas' model, it is assumed that the each gas species, once ionised and accelerated to the wall by the positively charged beam, will only desorbed molecules of the same species. For each species, the equations describing the evolution of the volume density, n, and surface density, θ, are the following:

$$\underbrace{V\frac{\partial n}{\partial t}}_{\substack{\text{time variation of}\\ \text{volumic density}\\ \text{in volume V per}\\ \text{unit length}}} = \underbrace{c_{spec}\frac{\partial^2 n}{\partial x^2}}_{\text{diffusion}} + \underbrace{\overbrace{\left(\eta_i + \eta'_i(\theta')\right)\ \sigma_{i-I}\frac{I}{e}\ n}^{\substack{\text{ions produced}\\ \text{by hadrons}}}}_{\text{ion-induced desorption}} - \underbrace{\sigma_{i-I}\frac{I}{e}\ n}_{\text{beam pumping}} - \underbrace{S_{wall}(\theta)n}_{\substack{\text{wall distributed}\\ \text{NEG pumping}}} - \underbrace{S_{cryo}\left(n - n_e(\theta', T)\right)}_{\substack{\text{wall distributed}\\ \text{cryo-pumping and}\\ \text{thermal equilibrium pressure}}}$$
$$+ \underbrace{\left(\eta_{ph} + \eta'_{ph}(\theta')\right)\dot{\Gamma}_{ph}}_{\substack{\text{photon stimulated}\\ \text{desorption}}} + \underbrace{\left(\eta_e + \eta'_e(\theta')\right)\dot{N}_e}_{\substack{\text{electron stimulated}\\ \text{desorption}}} + \underbrace{a \cdot q}_{\substack{\text{thermal}\\ \text{outgassing}}} \tag{1}$$

$$\underbrace{a\frac{\partial \theta}{\partial t}}_{\substack{\text{surface density}\\ \text{(on room temperature surfaces)}\\ \text{time variation}\\ \text{in the area A per}\\ \text{unit length}}} = \underbrace{S_{wall}(\theta)n}_{\substack{\text{wall distributed}\\ \text{NEG pumping}}} + \underbrace{\sigma_{i-I}\frac{I}{e}\ n}_{\text{beam pumping}} \tag{2}$$

$$\underbrace{a\frac{\partial \theta'}{\partial t}}_{\substack{\text{surface density}\\ \text{(on cold surfaces)}\\ \text{time variation}\\ \text{in the area A per}\\ \text{unit length}}} = S_{cryo}\left(n - n_e(\theta', T)\right) - \eta'_i(\theta')\sigma_{i-I}\frac{I}{e}n - \eta'_{ph}(\theta')\dot{\Gamma}_{ph} - \eta'_{ph}(\theta)\dot{N}_e \tag{3}$$

In a room temperature system, the physisorption can be neglected and the equation (1) reads:

$$V\frac{\partial n}{\partial t} = c_{spec}\frac{\partial^2 n}{\partial x^2} + (\eta_i - 1)\sigma_{i-I}\frac{I}{e}n - S_{wall}n - C_{dis}n + \eta_{ph}\dot{\Gamma}_{ph} + \eta_e\dot{N}_e + a \cdot q \tag{4}$$

Equation (4) stands also for a cryogenic system at equilibrium, when the surface density does not vary with time, adsorption and desorption from condensed layers balance out.

Legend:

- V = volume of the chamber per unit length [m^2];
- a = surface area of the chamber wall per unit length [m];
- $c_{spec} = area_{\substack{\text{cross}\\\text{section}}} \cdot Dif$, specific conductance per unit length [m^4/s]; (Dif = diffusion coefficient [m^2/s] [1])
- n = volume gas density [$1/m^3$];
- θ = gas surface density (or coverage) on ambient temperature surfaces [$1/m^2$];
- θ' = gas surface density (or coverage) on cryogenic surfaces [$1/m^2$];
- $v_{gas} = \sqrt{\frac{8k_BT}{\pi m_{gas}}}$, average molecular velocity for a Maxwell-Boltzmann distribution, function of the temperature T [K], the ion mass [kg] and the Boltzmann constant k_B [$kg.m^2/K.s^2$];
- $S_{wall} = \alpha(\theta)\frac{a \cdot v_{gas}}{4}$, [$m^2$/s] wall pumping speed (for example getter coating) at room temperature, per unit length ($\alpha =$ sticking coefficient at warm temperature and $\frac{a \cdot v_{gas}}{4}$ = molecular incident rate on the surface area a for a Maxwell-Boltzmann velocity distribution);
- $S_{cryo} = \alpha' \frac{a \cdot v_{gas}}{4}$, [$m^2$/s] wall pumping speed for condensation at cryogenic temperature, per unit length ($\alpha' =$ sticking coefficient at cryogenic temperature);
- n_e = thermal equilibrium density [molecules/m^3] (for cold surfaces, it corresponds to the vapour pressure at the temperature T);
- C_{dis} = wall pumping speed via holes (for example LHC beam screen holes) [m^2/s] per unit length.
- η and η' = ion (i), electron (e) and photon (ph) induced gas desorption coefficients from warm and cryogenic surfaces respectively;
- σ_{i-I} = ionisation cross section of the gas-hadron interaction [m^2];
- $\dot{\Gamma}_{ph}$ = photon flux to the wall per unit length [1/m/s];
- $\dot{N}_e$ = electron flux to the wall per unit length [1/m/s];
- q_{ph} = thermal outgassing per unit length [$1/m^2$/s];
- I = beam current [A];
- e = electron charge [C]

Remarks:

In the equations (1), (2) and (3) the ionisation of the residual gas via electron and photon interaction is neglected. The complete ion production term should be written as:

$$\left(\underbrace{\sigma_{i-I}\frac{I}{e}}_{\substack{\text{ions produced}\\\text{by hadrons}}} + \underbrace{\sigma_{i-e}\dot{N}_e}_{\substack{\text{ions produced}\\\text{by electrons}}} + \underbrace{\sigma_{i-ph}L\dot{\Gamma}_{ph}}_{\substack{\text{ions produced}\\\text{by photons}}} \right) \tag{5}$$

[1] Diffusion coefficient for a section of radius = $r(z)$ is given by $Dif = \frac{2}{3} v \cdot r(z)$

4. Multi-gas model

The dominant gas species present in a vacuum system are H_2, CH_4, CO and CO_2. The 'multi-gas' model takes into account that each of the gas species, once ionised, can desorb gas of any species both from the wall materials and from the condensed gas layers (in a cryogenic system). In the equation (1) for the general gas species '*gas*' the term representing the cross-desorption must be included:

$$\frac{I}{e}\sum_{\substack{other\\species\neq gas}}\left\{\left(\eta_{i,_{\substack{other\\species\to gas}}}+\eta'_{i,_{\substack{other\\species\to gas}}}(\theta'_{gas})\right)\sigma_{\substack{other\\species}}\cdot n_{\substack{other\\species}}\right\}\cdot$$

Hence, in this model, the equations for each species depend on the gas densities of other species, and all the equations result inter-dependent.

The set of equations to be solved for each of the gas species (in the example H_2 and CO_2) are given in equations (6) for the volumetric gas density and (7) for the surface gas density respectively.

$$\begin{cases}
V\dfrac{\partial n_{H_2}}{\partial t}=c_{spec,H_2}\cdot\ddot{n}_{H_2}\\
\quad+\dfrac{I}{e}\left(\eta_{i,H_2^+\to H_2}+\eta'_{i,H_2^+\to H_2}(\theta'_{H_2})-1\right)\sigma_{H_2}\cdot n_{H_2}+\dfrac{I}{e}\sum_{gas\neq H_2}\left\{\left(\eta_{i,gas^+-H_2}+\eta'_{i,gas^+-H_2}(\theta'_{H_2})\right)\sigma_{gas}\cdot n_{gas}\right\}\\
\quad-c_{w,H_2}\cdot\left(\alpha_{H_2}(\theta_{H_2})+\alpha'_{H_2}(\theta'_{H_2})\right)\cdot n_{H_2}+c_{w,H_2}\cdot\alpha'_{H_2}(\theta'_{H_2})\cdot n_{e,H_2}(\theta'_{H_2},T)-C_{H_2}\cdot n_{H_2}\\
\quad+\left(\eta_{ph,H_2}+\eta'_{ph,H_2}(\theta'_{H_2})\right)\cdot\dot{\Gamma}_{ph}+\left(\eta_{e,H_2}+\eta'_{e,H_2}(\theta'_{H_2})\right)\cdot\dot{N}_e+a\cdot q_{H_2}\\
..\\
V\dfrac{\partial n_{CO_2}}{\partial t}=c_{spec,CO_2}\cdot\ddot{n}_{CO_2}\\
\quad+\dfrac{I}{e}\left(\eta_{i,CO_2^+\to CO_2}+\eta'_{i,CO_2^+\to CO_2}(\theta'_{CO_2})-1\right)\sigma_{CO_2}\cdot n_{CO_2}+\dfrac{I}{e}\sum_{gas\neq CO_2}\left\{\left(\eta_{i,gas^+-CO_2}+\eta'_{i,gas^+-CO_2}(\theta'_{CO_2})\right)\sigma_{gas}\cdot n_{gas}\right.\\
\quad-c_{w,CO_2}\cdot\left(\alpha_{CO_2}(\theta_{CO_2})+\alpha'_{CO_2}(\theta'_{CO_2})\right)\cdot n_{CO_2}+c_{wCO_2}\cdot\alpha'_{CO_2}(\theta'_{CO_2})\cdot n_{e,CO_2}(\theta'_{CO_2},T)-C_{CO_2}\cdot n_{CO_2}\\
\quad+\left(\eta_{ph,CO_2}+\eta'_{ph,CO_2}(\theta'_{CO_2})\right)\cdot\dot{\Gamma}_{ph}+\left(\eta_{e,CO_2}+\eta'_{e,CO_2}(\theta'_{CO_2})\right)\cdot\dot{N}_e+a\cdot q_{CO_2}
\end{cases}\tag{6}$$

$$\begin{cases}
a\dfrac{\partial\theta_{H_2}}{\partial t}=\alpha_{H_2}(\theta_{H_2})\cdot c_{w,H_2}\cdot n_{H_2}+\dfrac{I}{e}\cdot\sigma_{H_2}\cdot n_{H_2}\\
..\\
a\dfrac{\partial\theta_{CO_2}}{\partial t}=\alpha_{CO_2}(\theta_{CO_2})\cdot c_{w,CO_2}\cdot n_{CO_2}+\dfrac{I}{e}\cdot\sigma_{CO_2}\cdot n_{CO_2}
\end{cases}\tag{7}$$

$$\begin{cases}
a\dfrac{\partial\theta'_{H_2}}{\partial t}=\alpha'_{H_2}(\theta'_{H_2})\cdot c_{wH_2}\cdot\left(n_{H_2}-n_{e,H_2}(\theta'_{H_2},T)\right)-\dfrac{I}{e}\cdot\eta'_{i,H_2^+\to H_2}(\theta'_{H_2})\cdot\sigma_{H_2}\cdot n_{H_2}\\
\quad-\dfrac{I}{e}\sum_{gas\neq H_2}\left\{\eta'_{i,gas^+\to H_2}(\theta'_{H_2})\cdot\sigma_{gas}\cdot n_{gas}\right\}-\eta'_{ph,H_2}(\theta'_{H_2})\cdot\dot{\Gamma}_{ph}-\eta'_{e,H_2}(\theta'_{H_2})\cdot\dot{N}_e;\\
..\\
a\dfrac{\partial\theta'_{CO_2}}{\partial t}=\alpha'_{CO_2}(\theta'_{CO_2})\cdot c_{w,CO_2}\cdot\left(n_{CO_2}-n_{e,CO_2}(\theta'_{CO_2},T)\right)-\dfrac{I}{e}\cdot\eta'_{i,CO_2^+\to CO_2}(\theta'_{CO_2})\cdot\sigma_{CO_2}\cdot n_{H_2}\\
\quad-\dfrac{I}{e}\sum_{gas\neq CO_2}\left\{\eta'_{i,gas^+\to CO_2}(\theta'_{gas})\cdot\sigma_{gas}\cdot n_{gas}\right\}-\eta'_{ph,CO_2}(\theta'_{CO_2})\cdot\dot{\Gamma}_{ph}-\eta'_{e,CO_2}(\theta'_{CO_2})\cdot\dot{N}_e;
\end{cases}\tag{8}$$

With $c_{wH_2}=\dfrac{a\cdot v_{H_2}}{4}$; $c_{wCO_2}=\dfrac{a\cdot v_{CO_2}}{4}$.

In the rest of this document it will be assumed to be at steady state, with a cryogenic system at equilibrium, and that the surface density in the warm sections varies very slowly with respect to the volume density. As a consequence, all the coefficients become time independent and the variation with time of volume density can be set to zero. The equations (6) read:

$$\begin{cases} V\dfrac{\partial n_{H_2}}{\partial t} = c_{spec,H_2}\cdot \ddot{n}_{H_2} + \dfrac{I}{e}\cdot\left(\eta_{i,H_2^+\to H_2}-1\right)\sigma_{H_2}\cdot n_{H_2} + \dfrac{I}{e}\sum_{gas\neq H_2}\left\{\eta_{i,gas^+-H_2}\cdot\sigma_{gas}\cdot n_{gas}\right\} \\ \qquad -c_{w,H_2}\cdot\alpha_{H_2}\cdot n_{H_2} - C_{H_2}\cdot n_{H_2} + \eta_{ph,H_2}\cdot\dot{\Gamma}_{ph} + \eta_{e,H_2}\cdot\dot{N}_e + a\cdot q_{H_2} \approx 0 \\ \ldots \\ V\dfrac{\partial n_{CO_2}}{\partial t} = c_{spec,CO_2}\cdot \ddot{n}_{CO_2} + \dfrac{I}{e}\cdot\left(\eta_{i,CO_2^+\to CO_2}-1\right)\sigma_{CO_2}\cdot n_{CO_2} + \dfrac{I}{e}\sum_{gas\neq CO_2}\left\{\eta_{i,gas^+-CO_2}\cdot\sigma_{gas}\cdot n_{gas}\right\} \\ \qquad -c_{w,CO_2}\cdot\alpha_{CO_2}\cdot n_{CO_2} - C_{CO_2}\cdot n_{CO_2} + \eta_{ph,CO_2}\cdot\dot{\Gamma}_{ph} + \eta_{e,CO_2}\cdot\dot{N}_e + a\cdot q_{CO_2} \approx 0 \end{cases} \tag{9}$$

5. Multi-gas model in matrix form

The set of equations (9) can be expressed in a more compact matrix form. To do so, we now define a set of vectors and matrices as follows:

Volume density [molecules·m^{-3}] and surface density (or coverage) in [molecules·m^{-2}]

$$\bar{n} = \begin{bmatrix} n_{H_2} \\ n_{CH_4} \\ n_{CO} \\ n_{CO_2} \end{bmatrix},\quad \bar{\theta} = \begin{bmatrix} \theta_{H_2} \\ \theta_{CH_4} \\ \theta_{CO} \\ \theta_{CO_2} \end{bmatrix} \text{ and } \bar{\theta'} = \begin{bmatrix} \theta'_{H_2} \\ \theta'_{CH_4} \\ \theta'_{CO} \\ \theta'_{CO_2} \end{bmatrix} \tag{10}$$

Thermal equilibrium density in [molecules·m^{-3}]

$$\bar{n}_e\left(\bar{\theta'},T\right) = \begin{bmatrix} n_{e,H_2}\left(\theta'_{H_2},T\right) \\ n_{e,CH_4}\left(\theta'_{CH_4},T\right) \\ n_{e,CO}\left(\theta'_{CO},T\right) \\ n_{e,CO_2}\left(\theta'_{CO_2},T\right) \end{bmatrix} \tag{11}$$

Specific conductance per unit length [m^4·s^{-1}]

$$\bar{\bar{A}} = \begin{bmatrix} c_{spec_{H_2}} & 0 & 0 & 0 \\ 0 & c_{spec_{CH_4}} & 0 & 0 \\ 0 & 0 & c_{spec_{CO}} & 0 \\ 0 & 0 & 0 & c_{spec_{CO_2}} \end{bmatrix} \tag{12}$$

Ionisation cross section in [m^2] by collision with ions or protons

$$\bar{\bar{\sigma}} = \begin{bmatrix} \sigma_{H_2} & 0 & 0 & 0 \\ 0 & \sigma_{CH_4} & 0 & 0 \\ 0 & 0 & \sigma_{CO} & 0 \\ 0 & 0 & 0 & \sigma_{CO_2} \end{bmatrix} \tag{13}$$

Ion induced desorption yields from the wall bulk material [molecules/ion]

$$\bar{\bar{\eta}}_i = \begin{bmatrix} \eta_{H_2^+-H_2} & \eta_{CH_4^+-H_2} & \eta_{CO^+-H_2} & \eta_{CO_2^+-H_2} \\ \eta_{H_2^+-CH_4} & \eta_{CH_4^+-CH_4} & \eta_{CO^+-CH_4} & \eta_{CO_2^+-CH_4} \\ \eta_{H_2^+-CO} & \eta_{CH_4^+-CO} & \eta_{CO^+-CO} & \eta_{CO_2^+-CO} \\ \eta_{H_2^+-CO_2} & \eta_{CH_4^+-CO_2} & \eta_{CO^+-CO_2} & \eta_{CO_2^+-CO_2} \end{bmatrix} \tag{14}$$

It should be noted that in the following of the document the beam pumping will not appear in the equations.

This means that one must take it into account when filling the input files. There are two possible ways of doing so: either set the values on the diagonal of $\bar{\bar{\eta}}_i$ equal to the desorption yields values and subtract 1 unit, or

calculate the equivalent pumping speed due to beam pumping for a given beam current, in units of $l \cdot s^{-1}$ and add that to the values in the $\overline{\overline{C_{bs}}}$ matrix (22).

Ion induced desorption yields physisorbed on cold surfaces [molecules/ion]

$$\overline{\overline{\eta'_i}}(\bar{\theta}) = \begin{bmatrix} \eta'_{H_2^+-H_2}(\theta'_{H_2}) & \eta'_{CH_4^+-H_2}(\theta'_{H_2}) & \eta'_{CO^+-H_2}(\theta'_{H_2}) & \eta'_{CO_2^+-H_2}(\theta'_{H_2}) \\ \eta'_{H_2^+-CH_4}(\theta'_{CH_4}) & \eta'_{CH_4^+-CH_4}(\theta'_{CH_4}) & \eta'_{CO^+-CH_4}(\theta'_{CH_4}) & \eta'_{CO_2^+-CH_4}(\theta'_{CH_4}) \\ \eta'_{H_2^+-CO}(\theta'_{CO}) & \eta'_{CH_4^+-CO}(\theta'_{CO}) & \eta'_{CO^+-CO}(\theta'_{CO}) & \eta'_{CO_2^+-CO}(\theta'_{CO}) \\ \eta'_{H_2^+-CO_2}(\theta'_{CO_2}) & \eta'_{CH_4^+-CO_2}(\theta'_{CO_2}) & \eta'_{CO^+-CO_2}(\theta'_{CO_2}) & \eta'_{CO_2^+-CO_2}(\theta'_{CO_2}) \end{bmatrix} \quad (15)$$

Electron induced desorption yields from the wall bulk material and physisorbed on cold surfaces respectively [molecules/electron]

$$\bar{\eta}_e = \begin{bmatrix} \eta_{e-H_2} \\ \eta_{e-CH_4} \\ \eta_{e-CO} \\ \eta_{e-CO_2} \end{bmatrix} \text{ and } \bar{\eta}'_e(\bar{\theta}) = \begin{bmatrix} \eta'_{e-H_2}(\theta'_{H_2}) \\ \eta'_{e-CH_4}(\theta'_{CH_4}) \\ \eta'_{e-CO}(\theta'_{CO}) \\ \eta'_{e-CO_2}(\theta'_{CO_2}) \end{bmatrix} \quad (16)$$

Photon induced desorption yields from the wall material and physisorbed on cold surfaces respectively [molecules/photon]

$$\bar{\eta}_{ph} = \begin{bmatrix} \eta_{ph-H_2} \\ \eta_{ph-CH_4} \\ \eta_{ph-CO} \\ \eta_{ph-CO_2} \end{bmatrix} \text{ and } \bar{\eta}'_{ph}(\bar{\theta}) = \begin{bmatrix} \eta'_{ph-H_2}(\theta'_{H_2}) \\ \eta'_{ph-CH_4}(\theta'_{CH_4}) \\ \eta'_{ph-CO}(\theta'_{CO}) \\ \eta'_{ph-CO_2}(\theta'_{CO_2}) \end{bmatrix} \quad (17)$$

Molecular mean velocity [$m \cdot s^{-1}$]

$$\overline{\overline{v}} = \sqrt{8k_B T/\pi} \begin{bmatrix} \sqrt{1/m_{H_2}} & 0 & 0 & 0 \\ 0 & \sqrt{1/m_{CH_4}} & 0 & 0 \\ 0 & 0 & \sqrt{1/m_{CO}} & 0 \\ 0 & 0 & 0 & \sqrt{1/m_{CO_2}} \end{bmatrix} \quad (18)$$

Linear pumping speed Beam screen hole conductance per unit length in [$m^3 \cdot s^{-1} \cdot m^{-1}$] ($C_{gas}$ in $l \cdot s^{-1} \cdot m^{-1}$)

$$\overline{\overline{C_{bs}}} = 10^{-3} \cdot \begin{bmatrix} C_{H_2} & 0 & 0 & 0 \\ 0 & C_{CH_4} & 0 & 0 \\ 0 & 0 & C_{CO} & 0 \\ 0 & 0 & 0 & C_{CO_2} \end{bmatrix} \quad (19)$$

Sticking coefficients on room temperature surfaces (NEG coating)

$$\overline{\overline{\alpha}}(\theta) = \begin{bmatrix} \alpha_{H_2}(\theta_{H_2}) & 0 & 0 & 0 \\ 0 & \alpha_{CH_4}(\theta_{CH_4}) & 0 & 0 \\ 0 & 0 & \alpha_{CO}(\theta_{CO}) & 0 \\ 0 & 0 & 0 & \alpha_{CO_2}(\theta_{CO_2}) \end{bmatrix} \quad (20)$$

Sticking coefficients on cryogenic temperature surfaces

$$\overline{\overline{\alpha'}}(\theta')=\begin{bmatrix} \alpha'_{H_2}(\theta'_{H_2}) & 0 & 0 & 0 \\ 0 & \alpha'_{CH_4}(\theta'_{CH_4}) & 0 & 0 \\ 0 & 0 & \alpha'_{CO}(\theta'_{CO}) & 0 \\ 0 & 0 & 0 & \alpha'_{CO_2}(\theta'_{CO_2}) \end{bmatrix} \tag{21}$$

Thermal outgassing rate in [molecules·s^{-1}·m^{-2}] (q_{gas} in torr·l·s^{-1}·cm^{-2})

$$\overline{Q_{th}}=\frac{1.33\cdot 10^{-5}}{k_B T}\begin{bmatrix} q_{H_2} \\ q_{CH_4} \\ q_{CO} \\ q_{CO_2} \end{bmatrix} \tag{22}$$

5.1. Fragmentation of the vacuum chambers into segments

A vacuum system can be composed by several elements (segments), each element being characterised by a different set of parameters. For each segment (identified by the index $k=1,N$) of generical geometry we define the following matrices:

$\overline{\overline{A}}_k$ specific conductance, already defined in (12), dependent only on the segment parameters [m^4·s^{-1}]

$$\overline{\overline{B}}_k=\left\{\frac{I}{e}\left(\overline{\overline{\eta}}_i^k+\overline{\overline{\eta}}'_i{}^k(\theta_k)\right)\overline{\overline{\sigma}}_k-\frac{a_k}{4}\cdot\overline{\overline{v}}_k\cdot\left(\overline{\overline{\alpha}}_k(\theta_k)+\overline{\overline{\alpha}}'_k(\theta_k)\right)-\overline{\overline{C_{bs}}}^k\right\} \tag{23}$$

dependent on the segment parameters (geometry, surface and temperature), and on the beam current [m^2·s^{-1}]

$$\overline{C}_k=\left\{\frac{a_k}{4}\overline{\overline{v}}_k\overline{\overline{\alpha}}'_k(\theta_k)\overline{n}_e^k(\theta_k,T_k)+\dot{N}_e^k\left(\overline{\eta}_e^k+\overline{\eta}'_e{}^k(\theta_k)\right)+\dot{\Gamma}^k_{ph}\left(\overline{\eta}^k_{ph}+\overline{\eta}'^k_{ph}(\theta_k)\right)+a_k\overline{Q_{th}}^k\right\} \tag{24}$$

dependent on the segment parameters (geometry, surface and temperature) and on the beam parameters [s^{-1}·m^{-1}]

In a cylindrical geometry of diameter d (mm), we can write:

$$a=10^{-3}\cdot\pi d \text{ [m]}$$
$$\overline{\overline{A}}_k=10^{-9}\cdot\frac{\pi d_k^3}{12}\cdot\overline{\overline{v}}_k \text{ [m}^4\text{·s}^{-1}\text{]} \tag{25}$$

In a conical geometry of diameters d_1 and d_2 and length L [mm], we can write:

$$a=10^{-3}\cdot\left[\pi\frac{d_{2,k}}{2}\sqrt{\left(\frac{d_{2,k}}{2}\right)^2+\left(\frac{d_{2,k}L}{d_{2,k}-d_{1,k}}\right)^2}-\pi\frac{d_{1,k}}{2}\sqrt{\left(\frac{d_{1,k}}{2}\right)^2+\left(\frac{d_{1,k}L}{d_{2,k}-d_{1,k}}\right)^2}\right] \text{ [m]}$$
$$\overline{\overline{A}}_k=10^{-9}\cdot\left[\frac{4\pi}{3}\left(\frac{d_{1,k}{}^2 d_{2,k}{}^2}{d_{1,k}+d_{2,k}}\right)\cdot\overline{\overline{v}}_k\right] \text{ [m}^4\text{·s}^{-1}\text{]} \tag{26}$$

In the assumption of quasi steady state, where the surface density varies with time much slower than the volume density, we can calculate the volume density from the equation (9), which in matrix form can be written as:

$$\overline{\overline{A}}_k\cdot\ddot{\overline{n}}_k+\overline{\overline{B}}_k\dot{\overline{n}}_k+\overline{C}_k\approx 0 \tag{27}$$

5.2. Boundary conditions

At the boundary between two segments the continuity of the density function must be guaranteed. Moreover, the sum of flux of molecules coming from the two side of one boundary must equal the amount of molecules pumped (S) or generated by a local source (g), as pictured in Figure 2.

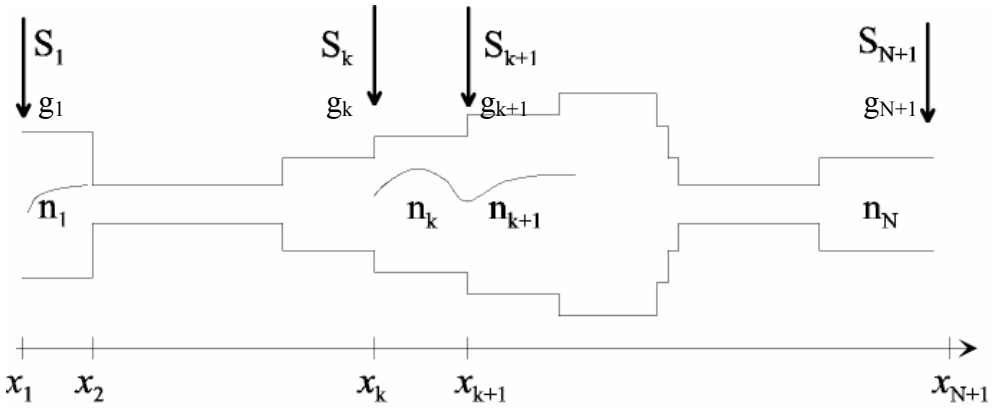

Figure 2 Schematic of a beam pipe. X_k = distance of the segment from a reference point.

$$\begin{aligned} \bar{n}_{k-1}(x_k) &= \bar{n}_k(x_k) \\ -\bar{\bar{A}}_{k-1}\dot{\bar{n}}_{k-1}(x_k) + \bar{\bar{A}}_k\dot{\bar{n}}_k(x_k) &= \bar{\bar{S}}_k\bar{n}_k(x_k) - \bar{g}_k \end{aligned} \qquad (28)$$

For *k=2,N*

Assuming an open pipe, where the pumping speed is equally shared between the two parts of the pipe, only half of the pumping speed at the extremities of the considered beam pipe section is available[2]:

$$\begin{aligned} \bar{\bar{A}}_1\dot{\bar{n}}_1(x_1) &= \bar{\bar{S}}_1/2\,\bar{n}_1(x_1) - \bar{g}_1 \\ -\bar{\bar{A}}_N\dot{\bar{n}}_N(x_{N+1}) &= \bar{\bar{S}}_{N+1}/2\,\bar{n}_N(x_{N+1}) - \bar{g}_{N+1} \end{aligned} \qquad (29)$$

For *k=1* and *k=N+1*

Where the matrices $\bar{\bar{S}}_k$ is the pumping speed [m^3/s] (*S* in l/s) and $\bar{g}_k$ is the localised gas source (*g* in [torr.l/s]) at the intersection between the segments (*k-1*) and (*k*)

$$\bar{\bar{S}}_k = 10^{-3}\cdot\begin{bmatrix} S_{H_2,k} & 0 & 0 & 0 \\ 0 & S_{CH_4,k} & 0 & 0 \\ 0 & 0 & S_{CO,k} & 0 \\ 0 & 0 & 0 & S_{CO_2,k} \end{bmatrix} \text{ and } \bar{g}_k = \frac{1.33\cdot 10^{-1}}{k_B T}\begin{bmatrix} g_{H_2,k} \\ g_{CH_4,k} \\ g_{CO,k} \\ g_{CO_2,k} \end{bmatrix} \qquad (30)$$

[2] With the above boundary conditions, only the solution of the density for known pumping speed at the pipe extremities can be found.

6. Transformation of the second order differential linear equation into a system of first orders equations

Each differential equation of the second order can be transformed, if linear, into two equations of the first order, with a change of variable. Let us call:

$$\begin{cases} \bar{y}_{1,k} = \bar{n}_k \\ \bar{y}_{2,k} = \dot{\bar{n}}_k \end{cases} \quad \text{For } k=1,N \tag{31}$$

The equation (27) becomes:

$$\begin{cases} \dot{\bar{y}}_{1,k} = \bar{y}_{2,k} \\ \dot{\bar{y}}_{2,k} = -\bar{\bar{A}}_k^{-1}\bar{\bar{B}}_k\bar{y}_{1,k} - \bar{\bar{A}}_k^{-1}\bar{C}_k \end{cases} \tag{32}$$

Where $\bar{\bar{I}}$ is the identity matrix.

We can now define the new matrices of matrices:

$$\bar{Y}_k = \begin{bmatrix} \bar{y}_{1,k} \\ \bar{y}_{2,k} \end{bmatrix} \tag{33}$$

$$\bar{\bar{M}}_k = \begin{bmatrix} \bar{\bar{0}} & \bar{\bar{I}} \\ -\bar{\bar{A}}_k^{-1}\bar{\bar{B}}_k & \bar{\bar{0}} \end{bmatrix} \text{ and } \bar{b}_k = \begin{bmatrix} \bar{\bar{0}} \\ -\bar{\bar{A}}_k^{-1}\bar{C}_k \end{bmatrix} \tag{34}$$

The equation (32) then becomes:

$$\dot{\bar{Y}}_k = \bar{\bar{M}}_k\bar{Y}_k + \bar{b}_k \tag{35}$$

Let z be the variable running along each segment $z \in [0 \quad L_k]$ where L_k represents the length of the segment k-th. The solution of equation (35) is given by:

$$\bar{Y}_k(z) = \exp\left(\bar{\bar{M}}_k z\right)\bar{Y}_{0,k} + \int_0^z \exp\left\{\bar{\bar{M}}_k(z-\tau)\right\}\bar{b}_k \, d\tau \tag{36}$$

$\bar{Y}_{0k} = \bar{Y}(z=0)$ represents the set of initial conditions

We define:

$$\begin{aligned} \bar{\bar{P}}_k(z) &= \exp\left(\bar{\bar{M}}_k z\right) \\ \bar{Q}_k(z) &= \int_0^z \exp\left\{\bar{\bar{M}}_k(z-\tau)\right\}\bar{b}_k \, d\tau \end{aligned} \tag{37}$$

We can write the solution as a function of the initial conditions:

$$\bar{Y}_k(z) = \bar{\bar{P}}_k(z)\bar{Y}_{0,k} + \bar{Q}_k(z) \tag{38}$$

6.1. Boundary conditions

The boundary conditions in equations (28) and (29) must now be expressed in terms of the new matrices:

$$\overline{\overline{H}}_{k-1}\overline{Y}_{k-1}(x_k)-\left(\overline{\overline{H}}_k+\overline{\overline{\Xi}}_k\right)\overline{Y}_k(x_k)=\overline{G}_k \tag{39}$$

For $k=2,N$

$$\overline{\overline{F}}_1\overline{Y}_1(x_1)=-\overline{g}_1$$

$$\overline{\overline{F}}_N\overline{Y}_N(x_{N+1})=\overline{g}_{N+1} \tag{40}$$

For $k=1$ and $k=N+1$

This can be derived if we write:

$$\begin{aligned}\overline{y}_{1,k-1}(x_k)&=\overline{y}_{1,k}(x_k)\\ -\overline{\overline{A}}_{k-1}\overline{y}_{2,k-1}(x_k)+\overline{\overline{A}}_k\overline{y}_{2,k}(x_k)&=\overline{\overline{S}}_k\overline{y}_{1,k}(x_k)-\overline{g}_k\end{aligned} \tag{41}$$

For $k=2,N$

$$\begin{aligned}-\frac{\overline{\overline{S}}_1}{2}\overline{y}_{1,1}(x_1)+\overline{\overline{A}}_1\overline{y}_{2,1}(x_1)&=-\overline{g}_1\\ \frac{\overline{\overline{S}}_{N+1}}{2}\overline{y}_{N,1}(x_{N+1})+\overline{\overline{A}}_N\overline{y}_{2,N}(x_{N+1})&=\overline{g}_{N+1}\end{aligned} \tag{42}$$

For $k=1$ and $k=N+1$

Defining:

$$\overline{\overline{H}}_k=\begin{bmatrix}\overline{\overline{I}} & \overline{\overline{0}}\\ \overline{\overline{0}} & -\overline{\overline{A}}_k\end{bmatrix},\quad \overline{\overline{\Xi}}_k=\begin{bmatrix}\overline{\overline{0}} & \overline{\overline{0}}\\ \overline{\overline{S}}_k & \overline{\overline{0}}\end{bmatrix}\ \text{and}\ \ \overline{G}_k=\begin{bmatrix}\overline{0}\\ -\overline{g}_k\end{bmatrix} \tag{43}$$

$$\overline{\overline{F}}_1=\begin{bmatrix}-\overline{\overline{S}}_1/2 & \overline{\overline{A}}_1\end{bmatrix}\ \text{and}\ \ \overline{\overline{F}}_N=\begin{bmatrix}\overline{\overline{S}}_{N+1}/2 & \overline{\overline{A}}_N\end{bmatrix} \tag{44}$$

7. Set of equations to be solved

The solution to the problem given in the equation (35) is given by the equation (38), where the values of $\overline{Y}_{0,k}$ can be calculated from the set of equations imposed by the boundary conditions. We want therefore to express such equations in terms of the initial conditions for each segment. Taking into account that at $z = L_{k-1}$, $\overline{Y}_{k-1}\left(L_{k-1}\right) = \overline{\overline{P}}_{k-1}\left(L_{k-1}\right)\overline{Y}_{0,k-1} + \overline{Q}_{k-1}\left(L_{k-1}\right)$ we finally get to the set of equations to be solved:

$$\overline{\overline{H}}_{k-1}\left[\overline{\overline{P}}_{k-1}\left(L_{k-1}\right)\overline{Y}_{0,k-1} + \overline{Q}_{k-1}\left(L_{k-1}\right)\right] - \left(\overline{\overline{H}}_{k} + \overline{\overline{\Xi}}_{k}\right)\overline{Y}_{0,k} = \overline{G}_{k} \qquad \text{For k=2,N} \tag{45}$$

$$\overline{\overline{F}}_{1}\overline{Y}_{0,1} = -\overline{g}_{1}$$

$$\overline{\overline{F}}_{N}\left[\overline{\overline{P}}_{N}\left(L_{N}\right)\overline{Y}_{0,N} + \overline{Q}_{N}\left(L_{N}\right)\right] = \overline{g}_{N+1} \qquad \text{For } k=1 \text{ and } k=N+1 \tag{46}$$

We can compact equations (45) and (46) together, and find a system of ($2\times N_{gas}\times N$) equations for the ($2\times N_{gas}\times N$) variables:

$$\begin{bmatrix} \overline{\overline{F}}_{1} & 0 & 0 & \cdots & 0 & 0 \\ \overline{\overline{H}}_{1}\overline{\overline{P}}_{1}(L_{1}) & -\left(\overline{\overline{H}}_{2}+\overline{\overline{\Xi}}_{2}\right) & 0 & \cdots & 0 & 0 \\ 0 & \overline{\overline{H}}_{2}\overline{\overline{P}}_{2}(L_{2}) & -\left(\overline{\overline{H}}_{3}+\overline{\overline{\Xi}}_{3}\right) & \cdots & 0 & 0 \\ 0 & \cdots & \cdots & \cdots & 0 & 0 \\ \cdots & \cdots & \cdots & \cdots & \cdots & \cdots \\ 0 & 0 & 0 & \cdots & \overline{\overline{H}}_{N-1}\overline{\overline{P}}_{N-1}(L_{N-1}) & -\left(\overline{\overline{H}}_{N}+\overline{\overline{\Xi}}_{N}\right) \\ 0 & 0 & 0 & \cdots & 0 & \overline{\overline{F}}_{N}\overline{\overline{P}}_{N}(L_{N}) \end{bmatrix} \begin{bmatrix} \overline{Y}_{0,1} \\ \overline{Y}_{0,2} \\ \overline{Y}_{0,3} \\ \cdots \\ \overline{Y}_{0,N-1} \\ \overline{Y}_{0,N} \end{bmatrix} = \begin{bmatrix} -\overline{g}_{1} \\ \overline{G}_{2} - \overline{\overline{H}}_{1}\overline{Q}_{1}(L_{1}) \\ \overline{G}_{3} - \overline{\overline{H}}_{2}\overline{Q}_{2}(L_{2}) \\ \cdots \\ \cdots \\ \overline{G}_{N} - \overline{\overline{H}}_{N-1}\overline{Q}_{N-1}(L_{N-1}) \\ \overline{g}_{N+1} - \overline{\overline{F}}_{N}\overline{Q}_{N}(L_{N}) \end{bmatrix} \tag{47}$$

$$\overline{\overline{Sm}} = \begin{bmatrix} \overline{\overline{F}}_{1} & 0 & 0 & \cdots & 0 & 0 \\ \overline{\overline{H}}_{1}\overline{\overline{P}}_{1}(L_{1}) & -\left(\overline{\overline{H}}_{2}+\overline{\overline{\Xi}}_{2}\right) & 0 & \cdots & 0 & 0 \\ 0 & \overline{\overline{H}}_{2}\overline{\overline{P}}_{2}(L_{2}) & -\left(\overline{\overline{H}}_{3}+\overline{\overline{\Xi}}_{3}\right) & \cdots & 0 & 0 \\ 0 & \cdots & \cdots & \cdots & 0 & 0 \\ \cdots & \cdots & \cdots & \cdots & \cdots & \cdots \\ 0 & 0 & 0 & \cdots & \overline{\overline{H}}_{N-1}\overline{\overline{P}}_{N-1}(L_{N-1}) & -\left(\overline{\overline{H}}_{N}+\overline{\overline{\Xi}}_{N}\right) \\ 0 & 0 & 0 & \cdots & 0 & \overline{\overline{F}}_{N}\overline{\overline{P}}_{N}(L_{N}) \end{bmatrix} \tag{48}$$

$$\overline{w} = \begin{bmatrix} -\overline{g}_{1} \\ \overline{G}_{2} - \overline{\overline{H}}_{1}\overline{Q}_{1}(L_{1}) \\ \overline{G}_{3} - \overline{\overline{H}}_{2}\overline{Q}_{2}(L_{2}) \\ \cdots \\ \cdots \\ \overline{G}_{N} - \overline{\overline{H}}_{N-1}\overline{Q}_{N-1}(L_{N-1}) \\ \overline{g}_{N+1} - \overline{\overline{F}}_{N}\overline{Q}_{N}(L_{N}) \end{bmatrix} \tag{49}$$

$$\overline{\overline{Sm}}\,\overline{Y}_{0} = \overline{w} \qquad \Rightarrow \qquad \overline{Y}_{0} = \overline{\overline{Sm}}^{-1}\overline{w} \tag{50}$$

8. Input file

The VASCO code is implemented in MATLAB. The input file must be a rectangular matrix without empty elements. The input parameter file structure is completely arbitrary, of course. The structure used for the VASCO code is shown in Figure 3.

Each vacuum chamber element occupies 4 columns, one per gas species taken into consideration. The input parameters are inserted per rows. The first row and 3 columns and the first row are invisible to the program, and their only purpose is to guide the preparation of the input file.

%			H2	CH4	CO	CO2	H2	CH4	CO	CO2	H2	CH4	CO	CO2
in_Segment = [		%	1	0	0	0	2	0	0	0	3	0	0	0
in_d = [	[mm]	%	100.00	0	0	0	100.00	0	0	0	42.28	0	0	0
in_L = [	[mm]	%	300.00	0	0	0	700.00	0	0	0	3866.00	0	0	0
in_dist_ref = [	[mm]	%	57972	0	0	0	58272	0	0	0	58972	0	0	0
in_T = [	[K]	%	300	0	0	0	300	0	0	0	300	0	0	0
in_S = [	[l/s] (H2)	%	0	0	0	0	0	0	0	0	50	0	0	0
	[l/s] (CH4)	%	0	0	0	0	0	0	0	0	0	30	0	0
	[l/s] (CO)	%	0	0	0	0	0	0	0	0	0	0	20	0
	[l/s] (CO2)	%	0	0	0	0	0	0	0	0	0	0	0	20
in_g = [	[torrl/s]	%	0	0	0	0	0	0	0	0	0	0	0	0
in_sigma = [	[m2]	%	4.45E-23	0	0	0	4.45E-23	0	0	0	4.45E-23	0	0	0
		%	0	3.18E-22	0	0	0	3.18E-22	0	0	0	3.18E-22	0	0
		%	0	0	2.75E-22	0	0	0	2.75E-22	0	0	0	2.75E-22	0
		%	0	0	0	4.29E-22	0	0	0	4.29E-22	0	0	0	4.29E-22
in_alpha = [		%	0	0	0	0	0	0	0	0	5.00E-03	0	0	0
		%	0	0	0	0	0	0	0	0	0	0.00E+00	0	0
		%	0	0	0	0	0	0	0	0	0	0	0.5	0
		%	0	0	0	0	0	0	0	0	0	0	0	0.5
in_alpha_p = [		%	0	0	0	0	0	0	0	0	0	0	0	0
		%	0	0	0	0	0	0	0	0	0	0	0	0
		%	0	0	0	0	0	0	0	0	0	0	0	0
		%	0	0	0	0	0	0	0	0	0	0	0	0
in_eta_i = [		%	0.54	0.54	0.54	0.54	0.54	0.54	0.54	0.54	0.05	0.05	0.05	0.05
		%	0.04	0.05	0.07	0.11	0.04	0.05	0.07	0.11	0.00	0.01	0.01	0.01
		%	0.25	0.29	0.29	0.33	0.25	0.29	0.29	0.33	0.03	0.03	0.03	0.03
		%	0.14	0.14	0.14	0.14	0.14	0.14	0.14	0.14	0.01	0.01	0.01	0.01
in_eta_p_i = [		%	0	0	0	0	0	0	0	0	0	0	0	0
		%	0	0	0	0	0	0	0	0	0	0	0	0
		%	0	0	0	0	0	0	0	0	0	0	0	0
		%	0	0	0	0	0	0	0	0	0	0	0	0
in_eta_e = [		%	1.77E-03	6.46E-05	4.52E-04	3.87E-04	1.77E-03	6.46E-05	4.52E-04	3.87E-04	3.33E-05	8.33E-07	1.67E-05	1.67E-05
in_eta_p_e = [		%	0	0	0	0	0	0	0	0	0	0	0	0
in_eta_ph = [		%	1.50E-04	4.00E-06	1.50E-05	2.50E-05	1.50E-04	4.00E-06	1.50E-05	2.50E-05	2.50E-07	2.50E-09	1.25E-08	1.25E-08
in_eta_p_ph = [		%	0	0	0	0	0	0	0	0	0	0	0	0
in_Cbs = [	[l/s/m]	%	0	0	0	0	0	0	0	0	0	0	0	0
		%	0	0	0	0	0	0	0	0	0	0	0	0
		%	0	0	0	0	0	0	0	0	0	0	0	0
		%	0	0	0	0	0	0	0	0	0	0	0	0
in_Qth = [		%	1.00E-12	5.00E-15	1.00E-14	5.00E-15	1.00E-12	5.00E-15	1.00E-14	5.00E-15	5.00E-14	3.00E-17	1.00E-14	1.00E-14
in_n_e = [		%	0	0	0	0	0	0	0	0	0	0	0	0
in_N_e = [	[e-/m/s]	%	1.2E+14	0	0	0	1.2E+14	0	0	0	6.0E+13	0	0	0
in_Gamma_ph	[ph/m/s]	%	3.0E+15	0	0	0	3.0E+15	0	0	0	3.0E+15	0	0	0
in_S_Nplus1 =	[l/s] (H2)	%	50	0	0	0	0	0	0	0	0	0	0	0
	[l/s] (CH4)	%	0	30	0	0	0	0	0	0	0	0	0	0
	[l/s] (CO)	%	0	0	20	0	0	0	0	0	0	0	0	0
	[l/s] (CO2)	%	0	0	0	20	0	0	0	0	0	0	0	0
in_g_Nplus1 =	[torrl/s]	%	0	0	0	0	0	0	0	0	0	0	0	0

Figure 3 Example of input file in the case of 3 segments

The first two segments represent uncoated sections at room temperature, the last segment has parameters typical of a NEG coated surface.

Parameters independent of gas species:

The parameters independent of gas species are placed in the H_2 column, and all the other columns are set equal to zero to fill the matrix. These parameters are:

- "in_Segment", in the 2nd row, contains the cardinal number corresponding to the segment. It is not used in the code, and can be chosen completely arbitrarily by the user.
- "in_d", in the 3rd row, contains the chamber diameter in that segment, expressed in mm.
- "in_L", in the 4th row, contains the length of that segment, expressed in mm.
- "in_dist_ref", in the 5th row, is the distance of the beginning of the segment from a chosen referent point, expressed in mm.
- "in_T", in the 6th row, contains the temperature of that segment, expressed in K.
- "in_N_e", in the 42nd row, contains the flux of electron hitting the wall along the segment, expressed in electrons·m^{-1}·s^{-1}. At present the code accepts only one value, which can correspond to a chosen energy of impact.
- in_Gamma_ph", in the 43rd row, contains the flux of photons hitting the wall along the segment, expressed in photons·m^{-1}·s^{-1}. At present the code accepts only one value, as in the previous case, which can correspond to a chosen energy of impact.

Lumped pumping and localised gas source:

- "in_S" (rows 7 to 10, and formulae (30)) is a matrix 4 times 4, representing the pumping speed (in l·s^{-1}) of a lumped pump (as seen at the beam axes) located on the left hand side of the segment. The elements to be filled lie on the diagonal of the matrix, in the positions (1,1) for the H_2 pumping speed, (2,2) for CH_4, (3,3) for CO and (4,4) for CO_2.
- "in_S_Nplus1" (rows 44 to 47) is a diagonal matrix 4 times 4, representing the pumping speed (in l·s^{-1}) of a lumped pump (as seen at the beam axes) located on the right hand side of the last segment. It can be non-zero only in the first columns of data (first segment even if it refers to the last segment) since the pumps on the right hand side of all the segments but last are also on the left hand side of the segment that follows.

In the example chosen for Figure 3 there is one lumped pumping group located between segment 2 and 3, and one on the right hand side of the 3rd segment. The matrices are highlighted in light green.

- "in_g" (row 11 and formulae (30)) is a vector composed by localised gas sources (in torr·l·s^{-1}) to take into account a leak or any kind of gas source located on the left hand side of the segment.
- "in_g_Nplus1" (row 48) is a vector composed by localised gas sources (in torr·l·s^{-1}) to take into consideration a leak or any kind of gas source located on the right hand side of the last segment. As for the lumped pumps, it can be non-zero only in the first columns of data (first segment even if it refers to the last segment) since gas sources on the right hand side of all the segments but last are also on the left hand side of the segment that follows.

Distributed pumping:

- "in_alpha" (rows 16 to 19, and formulae (20)) and "in_alpha_p" (rows 20 to 23) are diagonal matrices 4 times 4, filled with the sticking probability onto the surface of the segment at room temperature and cryogenic temperature, respectively. They represent, in the case of the LHC, the pumping due to NEG coating (chemisorption) in the warm sections, and to physisorption in the sections at cryogenic temperature. In the example, the three segments are at room temperature, so the sticking coefficient "in_alpha_p" is identically zero, and only the third segment has "in_alpha" non-zero since it is supposed to be NEG coated.
- "in_Cbs" (rows 36 to 39, and formula (19)) is a diagonal matrix 4 times 4, containing the pumping speed per unit length (in l·s^{-1}·m^{-1}), i.e. distributed along the segment. In the case of the LHC it represents the distributed pumping speed through the pumping slots of the beam screen in the cold magnets, or can be used to express any linear pumping speed, such as through later gaps in the collimators or in the LHCb VELO chamber.

Ionisation cross section:

- "in_sigma" (rows 12 to 15 and formula (13)) is a diagonal matrix 4 times 4, containing the ionisation cross section (in m^2) of molecules interacting with beam particles (protons or ions) at the beam circulating energy. In the example these matrices are highlighted in light blue.

Desorption yields:

- "in_eta_I" (rows 24 to 27) and "in_eta_p_I" (rows 28 to 31), formulae (14) and (15), are non-diagonal matrices 4 times 4, containing the ion stimulated desorption yields (in molecules per incident ion) at a chosen ion impact energy, at room temperature and cryogenic temperature, respectively.
- "in_eta_e" (row 32) and "in_eta_p_e" (row 33), formulae (16), are vectors containing the electron stimulated desorption yields (in molecules per incident electron) at chosen electron impact energy, at room temperature and cryogenic temperature, respectively.
- "in_eta_ph" (row 34) and "in_eta_p_ph" (row 35), formulae (17), are vectors containing the photon stimulated desorption yields (in molecules per incident photon) at chosen photon energy, at room temperature and cryogenic temperature, respectively.

Thermal outgassing:

- "in_Qth" (row 40), formula (22), is a vector containing the thermal outgassing rate per unit surface area (in torr·l·s^{-1}·cm^{-2}) at a chosen temperature.

Equilibrium pressure:

- "in_n_e" (row 41), formula (11), is a vector containing the equilibrium pressure at a given temperature (in torr) in a cryogenic system.

9. "Single-gas model": benchmark of the VASCO code against the PRESSURE code

To check the correctness of the VASCO calculations, the code results have been compared to the results of a different code, used previously for vacuum calculations [3], called PRESSURE. The latter is a code that can calculate pressure profiles (in torr) for a non-simple geometry. The pressure profile is calculated for one gas species at a time (single-gas model), imposing an approximated parabolic solution to the pressure equation. The PRESSURE code does not include contributions from photon and electron desorption. The two codes can be compared when the matrix $\overline{\overline{B}}$ of equation (27) is identically zero. In this case the parabolic solution is the correct solution.

The two cases chosen for the comparison are:

1) One segment with one lumped pump at each extremity, with the same pumping speed and thermal outgassing for all gas species. The ion induced desorption yields and distributed pumping are set to zero, so that the matrix $\overline{\overline{B}} = 0$. The photon and electron flux to the wall are also identically zero, since these contributions are not taken into account in the PRESSURE code. The input file is shown in Table 1 and the results are plotted in Figure 4.

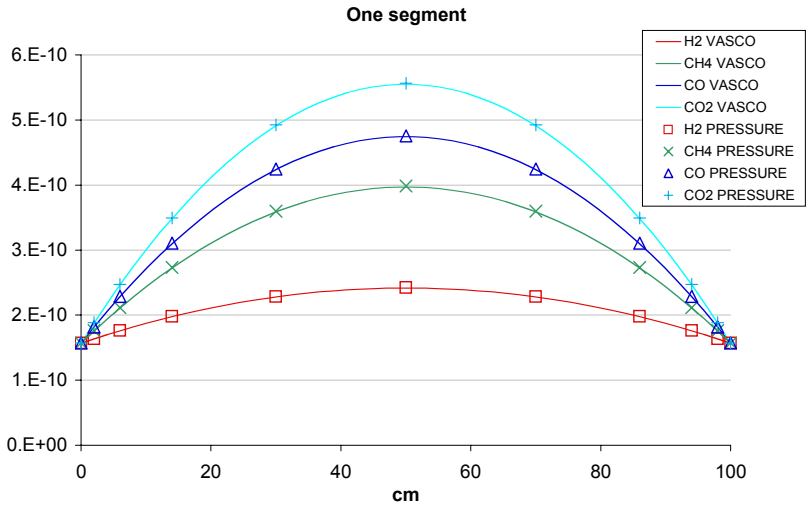

Figure 4 The results from the VASCO code, expressed in terms of pressure, are compared to the results of the PRESSURE code for the same input parameters and one segment.

It should be noted that the same case has been successfully validated against the analytical solution.

Table 1 - One segment

%			H2	CH4	CO	CO2
in_Segment = [		%	1	0	0	0
in_d = [	[mm]	%	100	0	0	0
in_L = [	[mm]	%	1000	0	0	0
in_dist_ref =	[mm]	%	1000	0	0	0
in_T = [	[K]	%	293	0	0	0
in_S = [	[l/s] (H2)	%	2000	0	0	0
	[l/s] (CH4)	%	0	2000	0	0
	[l/s] (CO)	%	0	0	2000	0
	[l/s] (CO2)	%	0	0	0	2000
in_g = [	[torrl/s]	%	0	0	0	0
in_sigma = [	[m2]	%	4.45E-23	0	0	0
		%	0	3.18E-22	0	0
		%	0	0	2.75E-22	0
		%	0	0	0	4.29E-22
in_alpha = [		%	0	0	0	0
		%	0	0	0	0
		%	0	0	0	0
		%	0	0	0	0
in_alpha_p = [		%	0	0	0	0
		%	0	0	0	0
		%	0	0	0	0
		%	0	0	0	0
in_eta_i = [		%	0	0	0	0
		%	0	0	0	0
		%	0	0	0	0
		%	0	0	0	0
in_eta_p_i = [		%	0	0	0	0
		%	0	0	0	0
		%	0	0	0	0
		%	0	0	0	0
in_eta_e = [		%	4.00E-04	2.00E-06	1.50E-04	3.00E-05
in_eta_p_e = [		%	0	0	0	0
in_eta_ph = [		%	1.50E-04	3.00E-06	1.50E-05	2.50E-05
in_eta_p_ph = [		%	0	0	0	0
in_Cbs = [	[l/s/m]	%	0	0	0	0
		%	0	0	0	0
		%	0	0	0	0
		%	0	0	0	0
in_Qth = [		%	1.00E-10	1.00E-10	1.00E-10	1.00E-10
in_n_e = [		%	0	0	0	0
in_N_e = [	[e-/m/s]	%	0.00E+00	0	0	0
in_Gamma_	[ph/m/s]	%	0.00E+00	0	0	0
in_S_Nplus1	[l/s] (H2)	%	2000	0	0	0
	[l/s] (CH4)	%	0	2000	0	0
	[l/s] (CO)	%	0	0	2000	0
	[l/s] (CO2)	%	0	0	0	2000
in_g_Nplus1	[torrl/s]	%	0	0	0	0

2) A sequence of 4 segments with increasing diameter, keeping the other parameters unchanged with respect to the previous case. The input file is shown in Table 2 and the results are presented in Figure 5.

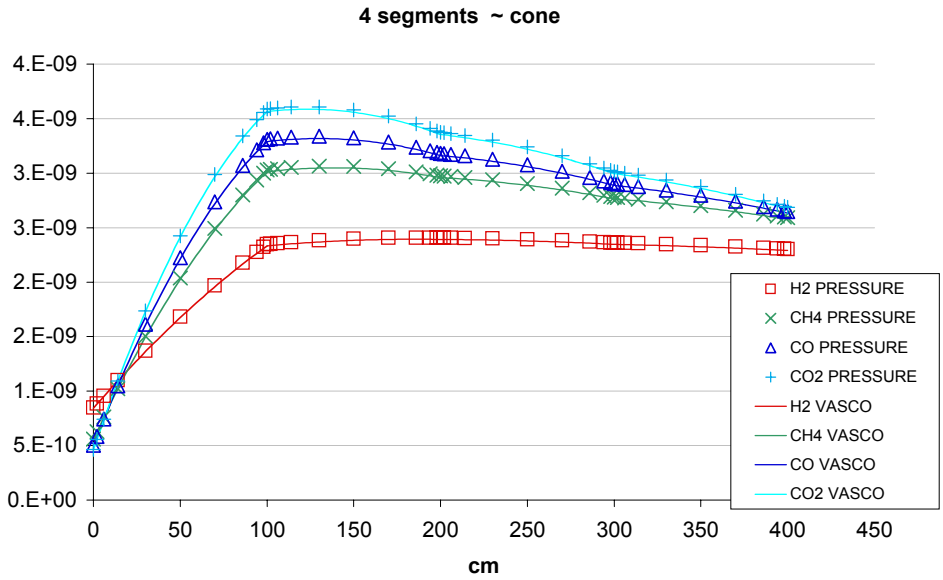

Figure 5 The results from the VASCO code, expressed in terms of pressure, are compared to the results of the PRESSURE code for the same input parameters and 4 segments of increasing diameter.

Table 2 - Add 3 segments between the two lumped pumps (4 segments in total) with increasing diameter (as highlighted in light blue)

%			H2	CH4	CO	CO2	H2	CH4	CO	CO2	H2	CH4	CO	CO2	H2	CH4	CO	CO2
in_Segment = [		%	1	0	0	0	2	0	0	0	3	0	0	0	4	0	0	0
in_d = [	[mm]	%	100	0	0	0	200	0	0	0	300	0	0	0	400	0	0	0
in_L = [	[mm]	%	1000	0	0	0	1000	0	0	0	1000	0	0	0	1000	0	0	0
in_dist_ref =	[mm]	%	1000	0	0	0	1000	0	0	0	1000	0	0	0	1000	0	0	0
in_T = [	[K]	%	293	0	0	0	293	0	0	0	293	0	0	0	293	0	0	0
in_S = [	[l/s] (H2)	%	2000	0	0	0	0	0	0	0	0	0	0	0	0	0	0	0
	[l/s] (CH4)	%	0	2000	0	0	0	0	0	0	0	0	0	0	0	0	0	0
	[l/s] (CO)	%	0	0	2000	0	0	0	0	0	0	0	0	0	0	0	0	0
	[l/s] (CO2)	%	0	0	0	2000	0	0	0	0	0	0	0	0	0	0	0	0
in_g = [	[torrl/s]	%	0	0	0	0	0	0	0	0	0	0	0	0	0	0	0	0
in_sigma =	[m2]	%	4.45E-23	0	0	0	4.45E-23	0	0	0	4.45E-23	0	0	0	4.45E-23	0	0	0
		%	0	3.18E-22	0	0	0	3.18E-22	0	0	0	3.18E-22	0	0	0	3.18E-22	0	0
		%	0	0	2.75E-22	0	0	0	2.75E-22	0	0	0	2.75E-22	0	0	0	2.75E-22	0
		%	0	0	0	4.29E-22	0	0	0	4.29E-22	0	0	0	4.29E-22	0	0	0	4.29E-22
in_alpha = [		%	0	0	0	0	0	0	0	0	0	0	0	0	0	0	0	0
		%	0	0	0	0	0	0	0	0	0	0	0	0	0	0	0	0
		%	0	0	0	0	0	0	0	0	0	0	0	0	0	0	0	0
		%	0	0	0	0	0	0	0	0	0	0	0	0	0	0	0	0
in_alpha_p = [		%	0	0	0	0	0	0	0	0	0	0	0	0	0	0	0	0
		%	0	0	0	0	0	0	0	0	0	0	0	0	0	0	0	0
		%	0	0	0	0	0	0	0	0	0	0	0	0	0	0	0	0
		%	0	0	0	0	0	0	0	0	0	0	0	0	0	0	0	0
in_eta_i = [		%	0	0	0	0	0	0	0	0	0	0	0	0	0	0	0	0
		%	0	0	0	0	0	0	0	0	0	0	0	0	0	0	0	0
		%	0	0	0	0	0	0	0	0	0	0	0	0	0	0	0	0
		%	0	0	0	0	0	0	0	0	0	0	0	0	0	0	0	0
in_eta_p_i = [		%	0	0	0	0	0	0	0	0	0	0	0	0	0	0	0	0
		%	0	0	0	0	0	0	0	0	0	0	0	0	0	0	0	0
		%	0	0	0	0	0	0	0	0	0	0	0	0	0	0	0	0
		%	0	0	0	0	0	0	0	0	0	0	0	0	0	0	0	0
in_eta_e = [		%	4.00E-04	2.00E-06	1.50E-04	3.00E-05	4.00E-04	2.00E-06	1.50E-04	3.00E-05	4.00E-04	2.00E-06	1.50E-04	3.00E-05	4.00E-04	2.00E-06	1.50E-04	3.00E-05
in_eta_p_e = [		%	0	0	0	0	0	0	0	0	0	0	0	0	0	0	0	0
in_eta_ph = [		%	1.50E-04	3.00E-06	1.50E-05	2.50E-05	1.50E-04	3.00E-06	1.50E-05	2.50E-05	1.50E-04	3.00E-06	1.50E-05	2.50E-05	1.50E-04	3.00E-06	1.50E-05	2.50E-05
in_eta_p_ph = [		%	0	0	0	0	0	0	0	0	0	0	0	0	0	0	0	0
in_Cbs = [	[l/s/m]	%	0	0	0	0	0	0	0	0	0	0	0	0	0	0	0	0
		%	0	0	0	0	0	0	0	0	0	0	0	0	0	0	0	0
		%	0	0	0	0	0	0	0	0	0	0	0	0	0	0	0	0
		%	0	0	0	0	0	0	0	0	0	0	0	0	0	0	0	0
in_Qth = [		%	1.00E-10	1.00E-10	1.00E-10	1.00E-10	1.00E-10	1.00E-10	1.00E-10	1.00E-10	1.00E-10	1.00E-10	1.00E-10	1.00E-10	1.00E-10	1.00E-10	1.00E-10	1.00E-10
in_n_e = [		%	0	0	0	0	0	0	0	0	0	0	0	0	0	0	0	0
in_N_e = [	[e-/m/s]	%	0.00E+00	0	0	0	0.00E+00	0	0	0	0.00E+00	0	0	0	0.00E+00	0	0	0
in_Gamma_	[ph/m/s]	%	0.00E+00	0	0	0	0.00E+00	0	0	0	0.00E+00	0	0	0	0.00E+00	0	0	0
in_S_Nplus	[l/s] (H2)	%	2000	0	0	0	0	0	0	0	0	0	0	0	0	0	0	0
	[l/s] (CH4)	%	0	2000	0	0	0	0	0	0	0	0	0	0	0	0	0	0
	[l/s] (CO)	%	0	0	2000	0	0	0	0	0	0	0	0	0	0	0	0	0
	[l/s] (CO2)	%	0	0	0	2000	0	0	0	0	0	0	0	0	0	0	0	0
in_g_Nplus	[torrl/s]	%	0	0	0	0	0	0	0	0	0	0	0	0	0	0	0	0

10. "Single-gas model" and "Multi-gas model": sensitivity of the models to parameters variation

The sensitivity of the models used in the VASCO program (single and multi-gas model) to parameter variation is studied and presented in this section. Several cases are analysed as summarised in Table 3. For all cases, the vacuum system is composed of two segments of same diameter and length, with three lumped pumps, two at the extremities and one between segments. The pumping speed is set to the same value for all gas species. The pump in the middle has half the pumping speed as the pumps at the extremities.

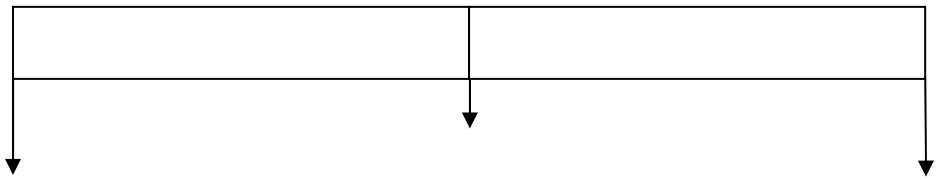

It should be noted that the parameters do not correspond to real cases (except for the last to cases considered), and are chosen to enhance the effect of variations. Moreover, given how the density is calculated, if all the sources independent of gas density (i.e. electron and photon induced desorption, thermal outgassing) are identically zero, only the banal solution is possible, since the vector $\overline{w} = \overline{0}$ (see equation (49)). Therefore, to analyse the effect of gas sources proportional to gas density (ion induced desorption), the other sources were set to a comparably very small number.

A large fraction of the tests focuses on the analysis of the variation of parameters affecting the matrix $\overline{\overline{B}}$ in the equation (27). This is because the major novelty of the VASCO code is the introduction of the multi-gas model, i.e. the cross interaction between gas species expressed by this matrix.

Table 3 - List of cases considered (the modification to the input parameters for different cases are highlighted in the corresponding tables)

CASE NUMBER and REFERENCE TABLE	**PARAMETER DESCRIPTION**	**CRITICAL CURRENT (A)**	**COMMENTS**
Case 1 Table 4	**Single-gas model** (matrix $\overline{\overline{\eta_i}}$ diagonal) with all parameters identical for all gas species, except the molecular mass (built in the program) and therefore the pipe conductance (calculated by the program).	**432.8**	The gas sources of photon and electron desorption are set to zero, while the thermal desorption is equal to a very small value, in order to put in evidence the effect of **variation of ionisation cross-sections** and **ion induced desorption yields,** and therefore of **variation of gas sources proportional to the gas density**.
Case 2 Table 5	**Single-gas model.** The ionisation cross-section values are changed and set equal to the values for proton at 7 Tev on different gas species. All the other parameters are unchanged with respect to Case 1.	**44.8**	
Case 3 Table 6	**Single-gas model.** Ion induced desorption yields half as in the Case 2, all the other parameters are left unchanged.	**89.7**	The effect of the **variation of ion induced desorption yields** by a factor of 2 should be less than the previous one, since ionisation cross-sections multiply ion induced desorption yields and were varied by larger factor. This case is introduced to be compared to the multi-gas model.

Case 4 Table 7	**Multi-gas model** (matrix $\overline{\overline{\eta_i}}$ non diagonal). All yields are set to the same value, i.e. =0.54 as used in Case 2.	**21.4**	The gas sources of photon and electron desorption are set to zero, while the thermal desorption is equal to a very small value, in order to put in evidence the effect of **variation of ion induced desorption yields** and therefore of **variation of gas sources proportional to the gas density**.
Case 5 Table 8	**Multi-gas model.** Ion induced desorption yields are set to half as in the Case 4. All the other parameters are left unchanged.	**42.8**	
Case 6 Table 9	**Multi-gas model.** Based on Case 4. The element in the 4th row and 4th column of the matrix $\overline{\overline{\eta_i}}$ (desorption of CO_2 molecules from CO_2 ion, $\eta_{CO_2^+-CO_2}$) is set = 1. All the other parameters are left unchanged.	**17.3**	
Case 7 Table 10	**Multi-gas model.** Based on Case 4. Vary element in the 1st row and 4th column (desorption of hydrogen molecules from CO_2 ion, $\eta_{CO_2^+-H_2}$) and element in the 4th row and 4th column ($\eta_{CO_2^+-CO_2}$) of the matrix $\overline{\overline{\eta_i}}$.	**17.2**	
Case 8 Table 11	**Multi-gas model.** Based on Case 4. Vary element in the 1st row and 4th column, 4th row-4th column and 4th row-1st column (desorption of CO_2 molecules from H_2 ion, $\eta_{H_2^+-CO_2}$) of the matrix $\overline{\overline{\eta_i}}$.	**17.1**	
Case 9 Table 12	**Multi-gas model.** Based on Case 4. Vary all elements in the 4th column (desorption of molecules from CO_2 ion).	**15.2**	
Case 10 Table 13	**Multi-gas model.** The values of ion induced desorption yield are taken from a real case (at ion incident energy of 300eV as expected in the LHC Long Straight Section in the absence of magnetic field).	**65.4**	
Case 11 Table 14	**Single-gas model.** Introduction of gas sources independent of gas density (to be compared to Case 2). All the other parameters are left unchanged.	**44.8**	**Variation of gas sources independent of gas density** analysed for some of the cases already seen previously. It can be noticed that, as expected, the critical current does not depend of sources independent of gas density.
Case 12 Table 15	**Multi-gas model.** Introduction of gas sources independent of gas density (to be compared to Case 4). All the other parameters are left unchanged.	**21.4**	
Case 13 Table 16	**Multi-gas model.** Gas sources independent of gas density are reduced by a factor of 100. All the other parameters are left unchanged.	**21.4**	
Case 14 Table 17	**Multi-gas model.** Introduction of gas sources independent of gas density (to be compared to Case 10). The values chosen for the desorption yields and for thermal outgassing correspond to a real case scenario.	**65.4**	**"Real cases":** the input parameters are the same as used for estimating the residual gas density in the LHC machine. The **variation of ion induced desorption yields** is analysed.
Case 16 Table 18	**Multi-gas model.** Change ion desorption yields with respect to Case 14.	**75.8**	

10.1. Variation of ionisation gas sources proportional to the gas density

In this section the variation of gas sources proportional to gas density, i.e. variation to the input parameters composing the matrix $\overline{\overline{B}}$ (equation (23)) is analysed both for the "single-gas" and the "multi-gas" models. The cases presented do not correspond to real cases and have been selected to highlight the role of the cross-correlation between gas species, given by the multi-gas model.

10.1.1. Single-gas model. Variation of ionisation cross-section values: comparison between Case 1 and 2

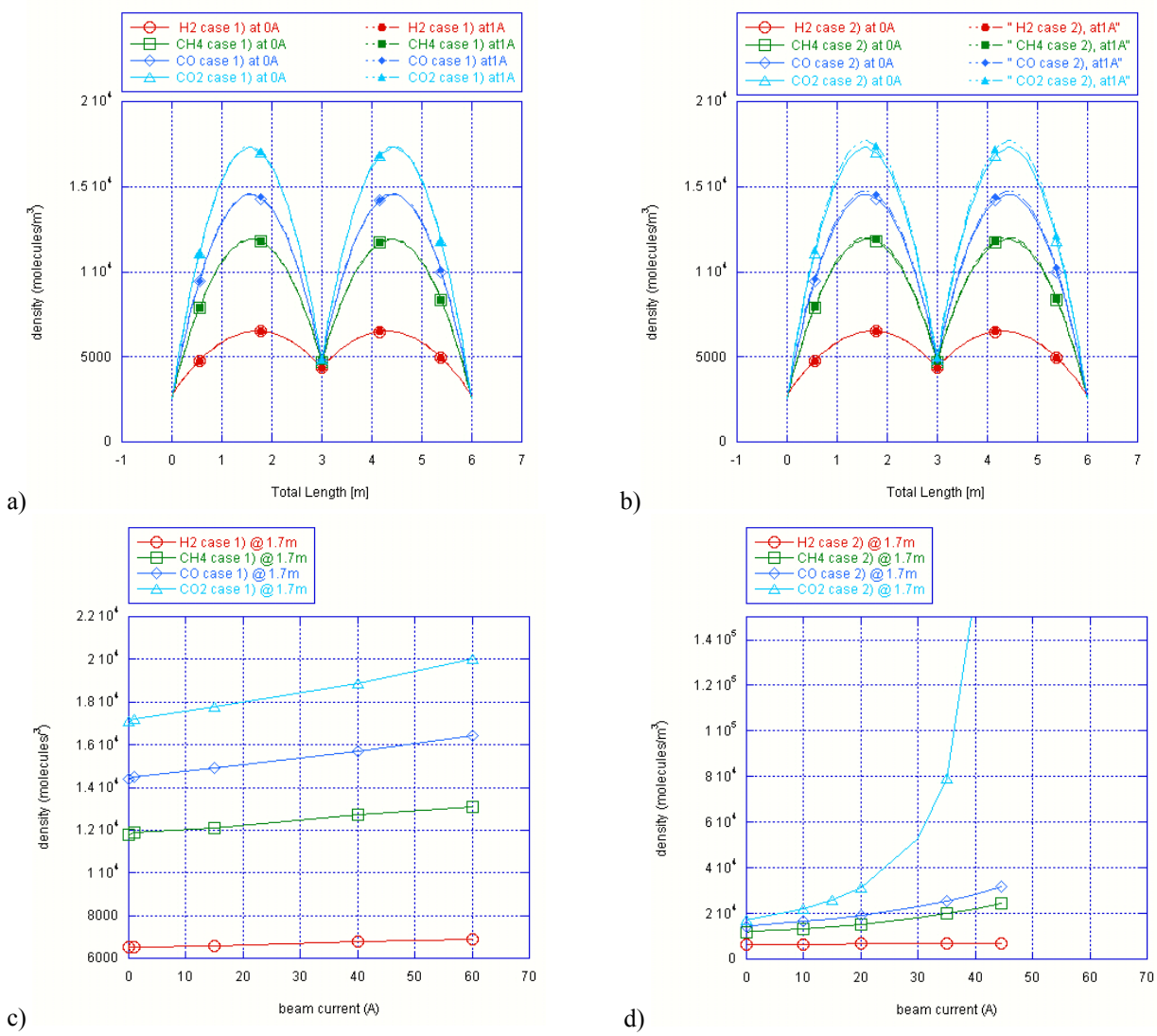

Figure 6 a) Density profile at 0 and 1A beam current for Case 1 (Table 4); b) Density profile at 0 and 1A beam current for Case 2 (Table 5); c) Density as a function of beam current for Case 1 at one location; d) Density as a function of beam current for Case 2 at one location (see also Figure 8)

Observations:

- Different gas species have different density profiles, due to their difference in mass, and therefore in molecular velocity and conductance.
- The ratio between the critical current in Case 1) and Case 2) is equal to the ratio between the ionisation cross-section values of CO_2. This is to be expected since when the input parameters are the same for all gas species (as in Case 1), the critical current will be limited by the gas with the lowest conductance, i.e. CO_2. In Case 2) the CO_2 ionisation cross-section is increased by the highest factor and the critical current will certainly be limited by CO_2 (as shown in *Figure 6* d, and *Figure 8*).
- The effect of the parameter variation depends on the beam current and on how close this is to the critical current, as illustrated in *Figure 6* c) and d). The ionisation cross-section for H_2 does not vary from Case 1)

to Case 2), and the results are therefore the same (ratio=1). For the other gas species, the ionisation cross-section is increased from Case 1) to Case 2a), as it is reflected in the higher density profile. The variation is the highest for CO_2 as shown in the evolution of gas density with beam current.

Table 4 - Case 1) Single-gas model: all parameters are the same for all gas species. Gas sources independent of gas density almost negligible

%			H2	CH4	CO	CO2	H2	CH4	CO	CO2
in_Segment = [		%	1	0	0	0	2	0	0	0
in_d = [	[mm]	%	91.63	0	0	0	91.63	0	0	0
in_L = [	[mm]	%	3000	0	0	0	3000	0	0	0
in_dist_ref = [	[mm]	%	3000	0	0	0	6000	0	0	0
in_T = [	[K]	%	300	0	0	0	300	0	0	0
in_S = [	[l/s] (H2)	%	1147.73	0	0	0	548.35	0	0	0
	[l/s] (CH4)	%	0	1147.73	0	0	0	548.35	0	0
	[l/s] (CO)	%	0	0	1147.73	0	0	0	548.35	0
	[l/s] (CO2)	%	0	0	0	1147.73	0	0	0	548.35
in_g = [	[torrl/s]	%	0	0	0	0	0	0	0	0
in_sigma = [	[m2]	%	4.45E-23	0	0	0	4.45E-23	0	0	0
		%	0	4.45E-23	0	0	0	4.45E-23	0	0
		%	0	0	4.45E-23	0	0	0	4.45E-23	0
		%	0	0	0	4.45E-23	0	0	0	4.45E-23
in_alpha = [		%	0	0	0	0	0	0	0	0
		%	0	0	0	0	0	0	0	0
		%	0	0	0	0	0	0	0	0
		%	0	0	0	0	0	0	0	0
in_alpha_p = [		%	0	0	0	0	0	0	0	0
		%	0	0	0	0	0	0	0	0
		%	0	0	0	0	0	0	0	0
		%	0	0	0	0	0	0	0	0
in_eta_i = [		%	0.54	0	0	0	0.54	0	0	0
		%	0	0.54	0	0	0	0.54	0	0
		%	0	0	0.54	0	0	0	0.54	0
		%	0	0	0	0.54	0	0	0	0.54
in_eta_p_i = [		%	0	0	0	0	0	0	0	0
		%	0	0	0	0	0	0	0	0
		%	0	0	0	0	0	0	0	0
		%	0	0	0	0	0	0	0	0
in_eta_e = [		%	1.77E-03	1.77E-03	1.77E-03	1.77E-03	1.77E-03	1.77E-03	1.77E-03	1.77E-03
in_eta_p_e = [		%	0	0	0	0	0	0	0	0
in_eta_ph = [		%	1.50E-04	1.50E-04	1.50E-04	1.50E-04	1.50E-04	1.50E-04	1.50E-04	1.50E-04
in_eta_p_ph = [		%	0	0	0	0	0	0	0	0
in_Cbs = [	[l/s/m]	%	0	0	0	0	0	0	0	0
		%	0	0	0	0	0	0	0	0
		%	0	0	0	0	0	0	0	0
		%	0	0	0	0	0	0	0	0
in_Qth = [		%	1.00E-20	1.00E-20	1.00E-20	1.00E-20	1.00E-20	1.00E-20	1.00E-20	1.00E-20
in_n_e = [		%	0	0	0	0	0	0	0	0
in_N_e = [	[e-/m/s]	%	0	0	0	0	0	0	0	0
in_Gamma_ph	[ph/m/s]	%	0	0	0	0	0	0	0	0
in_S_Nplus1 =	[l/s] (H2)	%	1147.73	0	0	0	0	0	0	0
	[l/s] (CH4)	%	0	1147.73	0	0	0	0	0	0
	[l/s] (CO)	%	0	0	1147.73	0	0	0	0	0
	[l/s] (CO2)	%	0	0	0	1147.73	0	0	0	0
in_g_Nplus1 =	[torrl/s]	%	0	0	0	0	0	0	0	0

Table 5 - Case 2) Variation of ionisation cross-section

%			H2	CH4	CO	CO2	H2	CH4	CO	CO2
in_Segment = [		%	1	0	0	0	2	0	0	0
in_d = [	[mm]	%	91.63	0	0	0	91.63	0	0	0
in_L = [	[mm]	%	3000	0	0	0	3000	0	0	0
in_dist_ref = [	[mm]	%	3000	0	0	0	6000	0	0	0
in_T = [	[K]	%	300	0	0	0	300	0	0	0
in_S = [	[l/s] (H2)	%	1147.73	0	0	0	548.35	0	0	0
	[l/s] (CH4)	%	0	1147.73	0	0	0	548.35	0	0
	[l/s] (CO)	%	0	0	1147.73	0	0	0	548.35	0
	[l/s] (CO2)	%	0	0	0	1147.73	0	0	0	548.35
in_g = [	[torrl/s]	%	0	0	0	0	0	0	0	0
in_sigma = [	[m2]	%	4.45E-23	0	0	0	4.45E-23	0	0	0
		%	0	3.18E-22	0	0	0	3.18E-22	0	0
		%	0	0	2.75E-22	0	0	0	2.75E-22	0
		%	0	0	0	4.29E-22	0	0	0	4.29E-22
in_alpha = [		%	0	0	0	0	0	0	0	0
		%	0	0	0	0	0	0	0	0
		%	0	0	0	0	0	0	0	0
		%	0	0	0	0	0	0	0	0
in_alpha_p = [		%	0	0	0	0	0	0	0	0
		%	0	0	0	0	0	0	0	0
		%	0	0	0	0	0	0	0	0
		%	0	0	0	0	0	0	0	0
in_eta_i = [		%	0.54	0	0	0	0.54	0	0	0
		%	0	0.54	0	0	0	0.54	0	0
		%	0	0	0.54	0	0	0	0.54	0
		%	0	0	0	0.54	0	0	0	0.54
in_eta_p_i = [		%	0	0	0	0	0	0	0	0
		%	0	0	0	0	0	0	0	0
		%	0	0	0	0	0	0	0	0
		%	0	0	0	0	0	0	0	0
in_eta_e = [		%	1.77E-03	1.77E-03	1.77E-03	1.77E-03	1.77E-03	1.77E-03	1.77E-03	1.77E-03
in_eta_p_e = [		%	0	0	0	0	0	0	0	0
in_eta_ph = [		%	1.50E-04	1.50E-04	1.50E-04	1.50E-04	1.50E-04	1.50E-04	1.50E-04	1.50E-04
in_eta_p_ph = [		%	0	0	0	0	0	0	0	0
in_Cbs = [	[l/s/m]	%	0	0	0	0	0	0	0	0
		%	0	0	0	0	0	0	0	0
		%	0	0	0	0	0	0	0	0
		%	0	0	0	0	0	0	0	0
in_Qth = [		%	1.00E-20	1.00E-20	1.00E-20	1.00E-20	1.00E-20	1.00E-20	1.00E-20	1.00E-20
in_n_e = [		%	0	0	0	0	0	0	0	0
in_N_e = [	[e-/m/s]	%	0	0	0	0	0	0	0	0
in_Gamma_ph	[ph/m/s]	%	0	0	0	0	0	0	0	0
in_S_Nplus1 =	[l/s] (H2)	%	1147.73	0	0	0	0	0	0	0
	[l/s] (CH4)	%	0	1147.73	0	0	0	0	0	0
	[l/s] (CO)	%	0	0	1147.73	0	0	0	0	0
	[l/s] (CO2)	%	0	0	0	1147.73	0	0	0	0
in_g_Nplus1 =	[torrl/s]	%	0	0	0	0	0	0	0	0

10.1.2. *Case 3) Single-gas model.* Ion induced gas desorption yields 1/2 as in Case 2. Comparison between Case 2 and 3

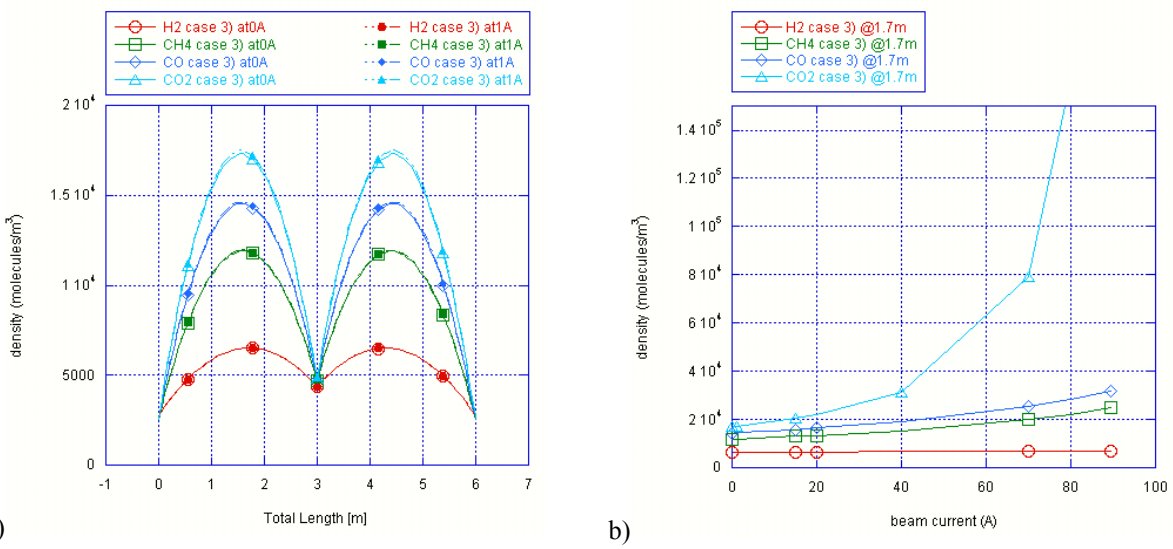

a) b)

Figure 7 a) Density profile at 0 and 1A beam current for Case 3 (Table 6); b) Density as a function of beam current for Case 3 at one location (see also Figure 8).

Observations:

- The variation between Case 2) and Case 3) is lower than in the previous comparison. In fact, the ionisation cross-section multiply the ion induced desorption yield, and the relative variation of their product is lower between Case 2) and Case 3) than between Case 1) and Case 2).

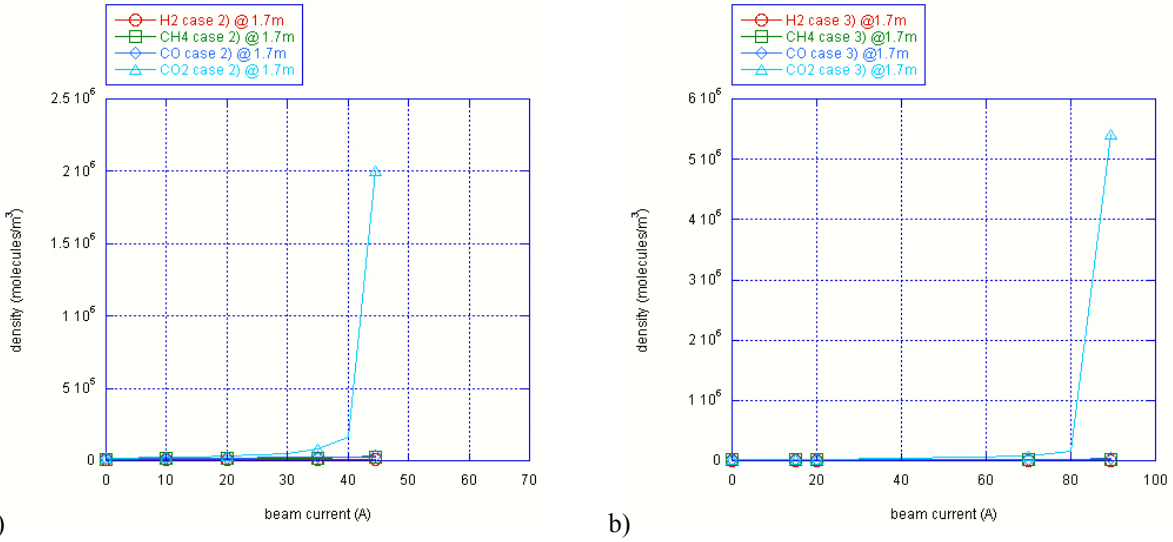

a) b)

Figure 8 a) Density as a function of beam current for Case 2 at one location.; b Density as a function of beam current for Case 3 at one location.

- The ratio between the critical current in Case 2) and Case 3) is equal to the ratio between the ion induced desorption yield values of CO_2. As in the previous case, this was expected. In *Figure 8* one can clearly see that the critical current is limited by CO_2 since the density of CO_2 diverges approaching the critical current value.
- Moreover, since the gas species in the single gas model are decoupled, the density of other gas species does not increase.

Table 6 - Case 3) Ion induced gas desorption yields 1/2 as in previous case

%			H2	CH4	CO	CO2	H2	CH4	CO	CO2
in_Segment = [		%	1	0	0	0	2	0	0	0
in_d = [	[mm]	%	91.63	0	0	0	91.63	0	0	0
in_L = [	[mm]	%	3000	0	0	0	3000	0	0	0
in_dist_ref = [	[mm]	%	3000	0	0	0	6000	0	0	0
in_T = [	[K]	%	300	0	0	0	300	0	0	0
in_S = [	[l/s] (H2)	%	1147.73	0	0	0	548.35	0	0	0
	[l/s] (CH4)	%	0	1147.73	0	0	0	548.35	0	0
	[l/s] (CO)	%	0	0	1147.73	0	0	0	548.35	0
	[l/s] (CO2)	%	0	0	0	1147.73	0	0	0	548.35
in_g = [	[torrl/s]	%	0	0	0	0	0	0	0	0
in_sigma = [	[m2]	%	4.45E-23	0	0	0	4.45E-23	0	0	0
		%	0	3.18E-22	0	0	0	3.18E-22	0	0
		%	0	0	2.75E-22	0	0	0	2.75E-22	0
		%	0	0	0	4.29E-22	0	0	0	4.29E-22
in_alpha = [		%	0	0	0	0	0	0	0	0
		%	0	0	0	0	0	0	0	0
		%	0	0	0	0	0	0	0	0
		%	0	0	0	0	0	0	0	0
in_alpha_p = [		%	0	0	0	0	0	0	0	0
		%	0	0	0	0	0	0	0	0
		%	0	0	0	0	0	0	0	0
		%	0	0	0	0	0	0	0	0
in_eta_i = [		%	0.27	0	0	0	0.27	0	0	0
		%	0	0.27	0	0	0	0.27	0	0
		%	0	0	0.27	0	0	0	0.27	0
		%	0	0	0	0.27	0	0	0	0.27
in_eta_p_i = [		%	0	0	0	0	0	0	0	0
		%	0	0	0	0	0	0	0	0
		%	0	0	0	0	0	0	0	0
		%	0	0	0	0	0	0	0	0
in_eta_e = [		%	1.77E-03	1.77E-03	1.77E-03	1.77E-03	1.77E-03	1.77E-03	1.77E-03	1.77E-03
in_eta_p_e = [		%	0	0	0	0	0	0	0	0
in_eta_ph = [		%	1.50E-04	1.50E-04	1.50E-04	1.50E-04	1.50E-04	1.50E-04	1.50E-04	1.50E-04
in_eta_p_ph = [		%	0	0	0	0	0	0	0	0
in_Cbs = [	[l/s/m]	%	0	0	0	0	0	0	0	0
		%	0	0	0	0	0	0	0	0
		%	0	0	0	0	0	0	0	0
		%	0	0	0	0	0	0	0	0
in_Qth = [		%	1.00E-20	1.00E-20	1.00E-20	1.00E-20	1.00E-20	1.00E-20	1.00E-20	1.00E-20
in_n_e = [		%	0	0	0	0	0	0	0	0
in_N_e = [	[e-/m/s]	%	0	0	0	0	0	0	0	0
in_Gamma_ph	[ph/m/s]	%	0	0	0	0	0	0	0	0
in_S_Nplus1 =	[l/s] (H2)	%	1147.73	0	0	0	0	0	0	0
	[l/s] (CH4)	%	0	1147.73	0	0	0	0	0	0
	[l/s] (CO)	%	0	0	1147.73	0	0	0	0	0
	[l/s] (CO2)	%	0	0	0	1147.73	0	0	0	0
in_g_Nplus1 =	[torrl/s]	%	0	0	0	0	0	0	0	0

10.1.3. *Case 4) Multi-gas model* (non-diagonal matrix $\overline{\overline{\eta_i}}$) with ion induced gas desorption yields as in Case 2. Comparison between multi-gas single-gas model

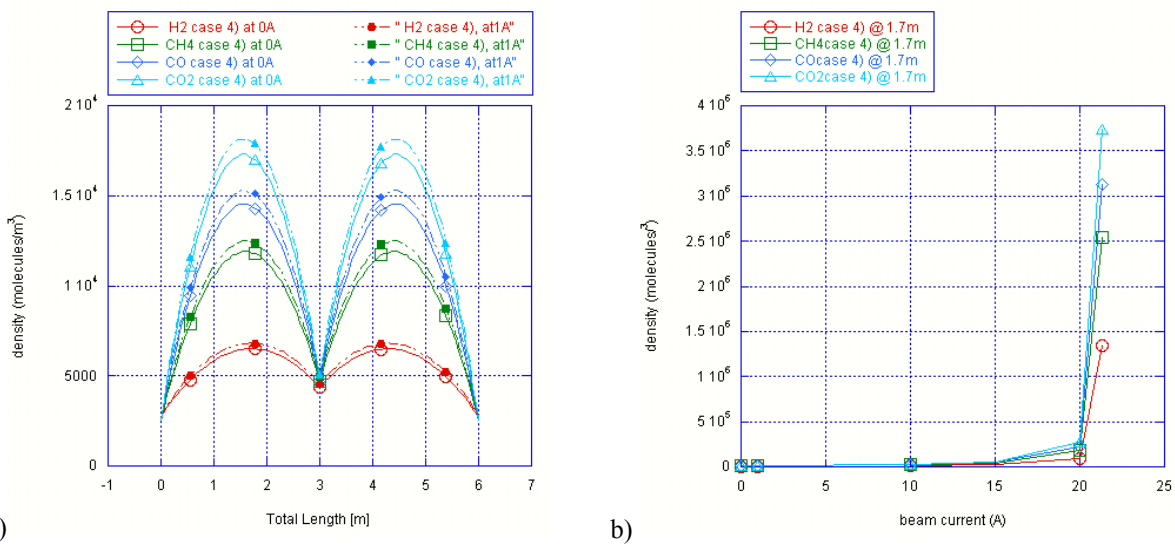

a) b)

Figure 9 a) Density profile at 0 and 1A beam current for Case 4 (Table 7); b) Density as a function of beam current for Case 4 at one location.

Observations:

- Also in Case 4 the critical current is limited by the ion induced CO_2, since all the parameters are the same for all gases except the conductance (lowest for CO_2) and the ionisation cross-section (highest for CO_2).
- The ratio between the critical current in Case 2) and Case 4) is about 2.1. In Case 4, the ion induced desorption term determining the critical current: $\frac{I}{e}\cdot\left(\eta_{i,CO_2\to CO_2}\cdot\sigma_{CO_2}\cdot n_{CO_2}+\sum_{gas\neq CO_2}\{\eta_{i,gas-CO_2}\cdot\sigma_{gas}\cdot n_{gas}\}\right)$, has become larger. If the gas density where all the same, the increment would be of 2.5 times.
- In this case one can see that all gas species are cross-correlated, since as the critical current is approached, all densities increase sharply.
- At beam current << than the critical current (in this case 1A) the gas density calculated in Case 4 and Case 2 do not differ very much (few percents).

Table 7 -Case 4) Multi-gas model (non-diagonal matrix $\overline{\overline{\eta_i}}$) with ion induced gas desorption yields as in Case 2

%			H2	CH4	CO	CO2	H2	CH4	CO	CO2
in_Segment = [		%	1	0	0	0	2	0	0	0
in_d = [	[mm]	%	91.63	0	0	0	91.63	0	0	0
in_L = [	[mm]	%	3000	0	0	0	3000	0	0	0
in_dist_ref = [	[mm]	%	3000	0	0	0	6000	0	0	0
in_T = [	[K]	%	300	0	0	0	300	0	0	0
in_S = [	[l/s] (H2)	%	1147.73	0	0	0	548.35	0	0	0
	[l/s] (CH4)	%	0	1147.73	0	0	0	548.35	0	0
	[l/s] (CO)	%	0	0	1147.73	0	0	0	548.35	0
	[l/s] (CO2)	%	0	0	0	1147.73	0	0	0	548.35
in_g = [	[torrl/s]	%	0	0	0	0	0	0	0	0
in_sigma = [	[m2]	%	4.45E-23	0	0	0	4.45E-23	0	0	0
		%	0	3.18E-22	0	0	0	3.18E-22	0	0
		%	0	0	2.75E-22	0	0	0	2.75E-22	0
		%	0	0	0	4.29E-22	0	0	0	4.29E-22
in_alpha = [		%	0	0	0	0	0	0	0	0
		%	0	0	0	0	0	0	0	0
		%	0	0	0	0	0	0	0	0
		%	0	0	0	0	0	0	0	0
in_alpha_p = [		%	0	0	0	0	0	0	0	0
		%	0	0	0	0	0	0	0	0
		%	0	0	0	0	0	0	0	0
		%	0	0	0	0	0	0	0	0
in_eta_i = [		%	0.54	0.54	0.54	0.54	0.54	0.54	0.54	0.54
		%	0.54	0.54	0.54	0.54	0.54	0.54	0.54	0.54
		%	0.54	0.54	0.54	0.54	0.54	0.54	0.54	0.54
		%	0.54	0.54	0.54	0.54	0.54	0.54	0.54	0.54
in_eta_p_i = [		%	0	0	0	0	0	0	0	0
		%	0	0	0	0	0	0	0	0
		%	0	0	0	0	0	0	0	0
		%	0	0	0	0	0	0	0	0
in_eta_e = [		%	1.77E-03	1.77E-03	1.77E-03	1.77E-03	1.77E-03	1.77E-03	1.77E-03	1.77E-03
in_eta_p_e = [		%	0	0	0	0	0	0	0	0
in_eta_ph = [		%	1.50E-04	1.50E-04	1.50E-04	1.50E-04	1.50E-04	1.50E-04	1.50E-04	1.50E-04
in_eta_p_ph = [		%	0	0	0	0	0	0	0	0
in_Cbs = [	[l/s/m]	%	0	0	0	0	0	0	0	0
		%	0	0	0	0	0	0	0	0
		%	0	0	0	0	0	0	0	0
		%	0	0	0	0	0	0	0	0
in_Qth = [		%	1.00E-20	1.00E-20	1.00E-20	1.00E-20	1.00E-20	1.00E-20	1.00E-20	1.00E-20
in_n_e = [		%	0	0	0	0	0	0	0	0
in_N_e = [	[e-/m/s]	%	0	0	0	0	0	0	0	0
in_Gamma_ph	[ph/m/s]	%	0	0	0	0	0	0	0	0
in_S_Nplus1 =	[l/s] (H2)	%	1147.73	0	0	0	0	0	0	0
	[l/s] (CH4)	%	0	1147.73	0	0	0	0	0	0
	[l/s] (CO)	%	0	0	1147.73	0	0	0	0	0
	[l/s] (CO2)	%	0	0	0	1147.73	0	0	0	0
in_g_Nplus1 =	[torrl/s]	%	0	0	0	0	0	0	0	0

10.1.4. *Case 5) Multi-gas model*. Ion induced gas desorption yields 1/2 as in Case 4

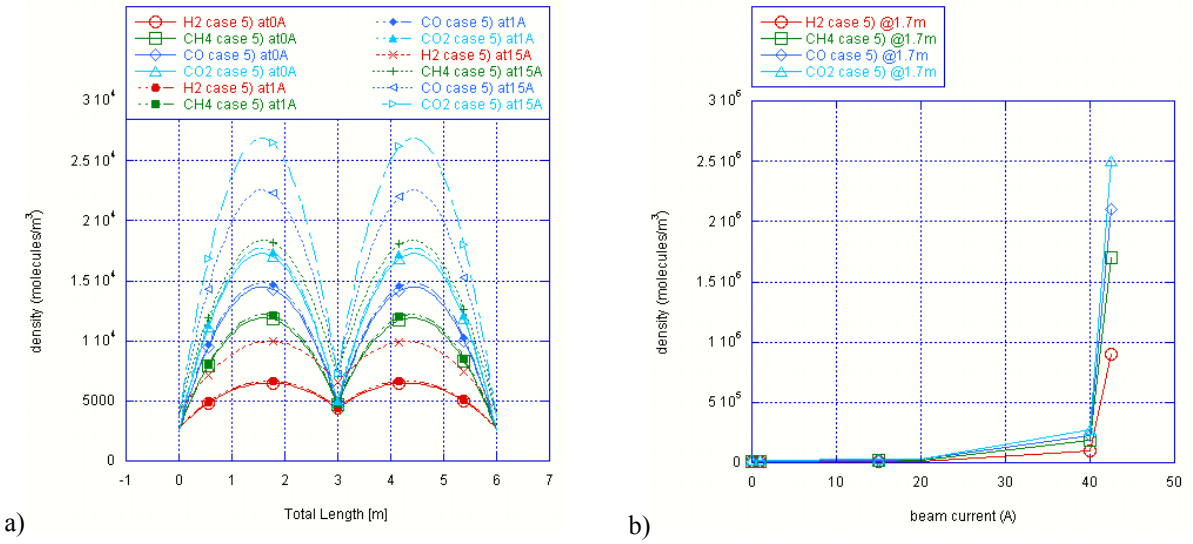

a) b)

Figure 10 a) Density profile at 0, 1 and 15A beam current for Case 5 (Table 8); b) Density as a function of beam current for Case 5 at one location.

Observations:

The same observations as before hold:

- The ratio between the critical current in Case 4) and Case 5) is a factor of 2 and equals the ratio between the ion induced desorption yields values of CO_2, which also in this case is the dominant gas, as shown in the figure above.
- For beam current << than the critical current, the gas density calculated in Case 5 is not far from previous cases, while it rapidly changes as the critical current is approached, that is as the contribution of ion induced desorption and the effect of avalanche becomes more important.

Table 8 - Case 5) Ion induced gas desorption yields 1/2 as in previous case

%			H2	CH4	CO	CO2	H2	CH4	CO	CO2
in_Segment = [		%	1	0	0	0	2	0	0	0
in_d = [	[mm]	%	91.63	0	0	0	91.63	0	0	0
in_L = [	[mm]	%	3000	0	0	0	3000	0	0	0
in_dist_ref = [	[mm]	%	3000	0	0	0	6000	0	0	0
in_T = [	[K]	%	300	0	0	0	300	0	0	0
in_S = [	[l/s] (H2)	%	1147.73	0	0	0	548.35	0	0	0
	[l/s] (CH4)	%	0	1147.73	0	0	0	548.35	0	0
	[l/s] (CO)	%	0	0	1147.73	0	0	0	548.35	0
	[l/s] (CO2)	%	0	0	0	1147.73	0	0	0	548.35
in_g = [	[torrl/s]	%	0	0	0	0	0	0	0	0
in_sigma = [	[m2]	%	4.45E-23	0	0	0	4.45E-23	0	0	0
		%	0	3.18E-22	0	0	0	3.18E-22	0	0
		%	0	0	2.75E-22	0	0	0	2.75E-22	0
		%	0	0	0	4.29E-22	0	0	0	4.29E-22
in_alpha = [		%	0	0	0	0	0	0	0	0
		%	0	0	0	0	0	0	0	0
		%	0	0	0	0	0	0	0	0
		%	0	0	0	0	0	0	0	0
in_alpha_p = [		%	0	0	0	0	0	0	0	0
		%	0	0	0	0	0	0	0	0
		%	0	0	0	0	0	0	0	0
		%	0	0	0	0	0	0	0	0
in_eta_i = [		%	0.27	0.27	0.27	0.27	0.27	0.27	0.27	0.27
		%	0.27	0.27	0.27	0.27	0.27	0.27	0.27	0.27
		%	0.27	0.27	0.27	0.27	0.27	0.27	0.27	0.27
		%	0.27	0.27	0.27	0.27	0.27	0.27	0.27	0.27
in_eta_p_i = [		%	0	0	0	0	0	0	0	0
		%	0	0	0	0	0	0	0	0
		%	0	0	0	0	0	0	0	0
		%	0	0	0	0	0	0	0	0
in_eta_e = [		%	1.77E-03	1.77E-03	1.77E-03	1.77E-03	1.77E-03	1.77E-03	1.77E-03	1.77E-03
in_eta_p_e = [		%	0	0	0	0	0	0	0	0
in_eta_ph = [		%	1.50E-04	1.50E-04	1.50E-04	1.50E-04	1.50E-04	1.50E-04	1.50E-04	1.50E-04
in_eta_p_ph = [		%	0	0	0	0	0	0	0	0
in_Cbs = [	[l/s/m]	%	0	0	0	0	0	0	0	0
		%	0	0	0	0	0	0	0	0
		%	0	0	0	0	0	0	0	0
		%	0	0	0	0	0	0	0	0
in_Qth = [		%	1.00E-20	1.00E-20	1.00E-20	1.00E-20	1.00E-20	1.00E-20	1.00E-20	1.00E-20
in_n_e = [		%	0	0	0	0	0	0	0	0
in_N_e = [	[e-/m/s]	%	0	0	0	0	0	0	0	0
in_Gamma_ph	[ph/m/s]	%	0	0	0	0	0	0	0	0
in_S_Nplus1 =	[l/s] (H2)	%	1147.73	0	0	0	0	0	0	0
	[l/s] (CH4)	%	0	1147.73	0	0	0	0	0	0
	[l/s] (CO)	%	0	0	1147.73	0	0	0	0	0
	[l/s] (CO2)	%	0	0	0	1147.73	0	0	0	0
in_g_Nplus1 =	[torrl/s]	%	0	0	0	0	0	0	0	0

10.1.5. *Case 6) Multi-gas model.* Change ion induced gas desorption yield $\eta_{CO_2^+-CO_2}$. Comparison between Case 4 and 6

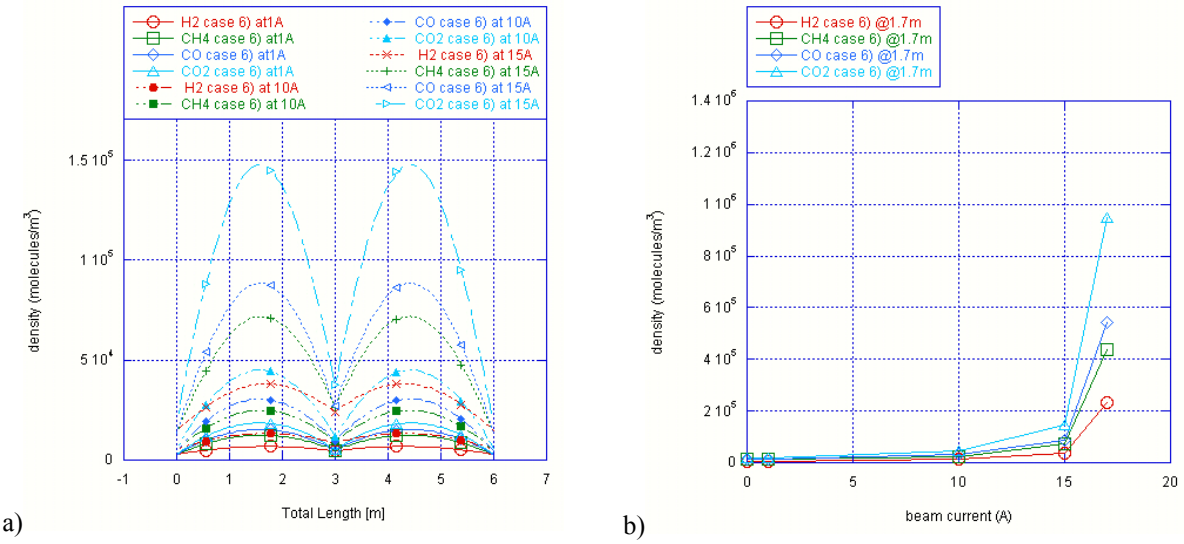

a) b)

Figure 11 a) Density profile at 1 and 15A beam current for Case 6 (Table 9); b) Density as a function of beam current for Case 6 at one location.

Observations:

- In Case 6 (*Figure 11* b), as before, the critical current is limited by CO_2. The ratio between the critical current in Case 4) and Case 6) is about 1.23. In Case 6, the ion induced desorption term determining the critical current: $\frac{I}{e}\cdot\left(\eta_{i,CO_2^+\rightarrow CO_2}\cdot\sigma_{CO_2}\cdot n_{CO_2}+\sum_{gas\neq CO_2}\left\{\eta_{i,gas^+-CO_2}\cdot\sigma_{gas}\cdot n_{gas}\right\}\right)$, has become larger than in Case 4. If the gas density where all the same, the increment would be of 1.34.
- Comparing the evolution of the density with beam current (*Figure 15* a), one can see that due to cross-desorption all gas species are affected by the increment of $\eta_{CO_2^+-CO_2}$, since they all increase faster than in Case 4.

Table 9 - Case 6) Change ion induced gas desorption yield $\eta_{CO_2^+-CO_2}=1$

%			H2	CH4	CO	CO2	H2	CH4	CO	CO2
in_Segment = [		%	1	0	0	0	2	0	0	0
in_d = [	[mm]	%	91.63	0	0	0	91.63	0	0	0
in_L = [	[mm]	%	3000	0	0	0	3000	0	0	0
in_dist_ref = [	[mm]	%	3000	0	0	0	6000	0	0	0
in_T = [	[K]	%	300	0	0	0	300	0	0	0
in_S = [	[l/s] (H2)	%	1147.73	0	0	0	548.35	0	0	0
	[l/s] (CH4)	%	0	1147.73	0	0	0	548.35	0	0
	[l/s] (CO)	%	0	0	1147.73	0	0	0	548.35	0
	[l/s] (CO2)	%	0	0	0	1147.73	0	0	0	548.35
in_g = [	[torrl/s]	%	0	0	0	0	0	0	0	0
in_sigma = [	[m2]	%	4.45E-23	0	0	0	4.45E-23	0	0	0
		%	0	3.18E-22	0	0	0	3.18E-22	0	0
		%	0	0	2.75E-22	0	0	0	2.75E-22	0
		%	0	0	0	4.29E-22	0	0	0	4.29E-22
in_alpha = [		%	0	0	0	0	0	0	0	0
		%	0	0	0	0	0	0	0	0
		%	0	0	0	0	0	0	0	0
		%	0	0	0	0	0	0	0	0
in_alpha_p = [		%	0	0	0	0	0	0	0	0
		%	0	0	0	0	0	0	0	0
		%	0	0	0	0	0	0	0	0
		%	0	0	0	0	0	0	0	0
in_eta_i = [		%	0.54	0.54	0.54	0.54	0.54	0.54	0.54	0.54
		%	0.54	0.54	0.54	0.54	0.54	0.54	0.54	0.54
		%	0.54	0.54	0.54	0.54	0.54	0.54	0.54	0.54
		%	0.54	0.54	0.54	1	0.54	0.54	0.54	1
in_eta_p_i = [		%	0	0	0	0	0	0	0	0
		%	0	0	0	0	0	0	0	0
		%	0	0	0	0	0	0	0	0
		%	0	0	0	0	0	0	0	0
in_eta_e = [		%	1.77E-03	1.77E-03	1.77E-03	1.77E-03	1.77E-03	1.77E-03	1.77E-03	1.77E-03
in_eta_p_e = [		%	0	0	0	0	0	0	0	0
in_eta_ph = [		%	1.50E-04	1.50E-04	1.50E-04	1.50E-04	1.50E-04	1.50E-04	1.50E-04	1.50E-04
in_eta_p_ph = [		%	0	0	0	0	0	0	0	0
in_Cbs = [	[l/s/m]	%	0	0	0	0	0	0	0	0
		%	0	0	0	0	0	0	0	0
		%	0	0	0	0	0	0	0	0
		%	0	0	0	0	0	0	0	0
in_Qth = [		%	1.00E-20	1.00E-20	1.00E-20	1.00E-20	1.00E-20	1.00E-20	1.00E-20	1.00E-20
in_n_e = [		%	0	0	0	0	0	0	0	0
in_N_e = [	[e-/m/s]	%	0	0	0	0	0	0	0	0
in_Gamma_ph	[ph/m/s]	%	0	0	0	0	0	0	0	0
in_S_Nplus1 =	[l/s] (H2)	%	1147.73	0	0	0	0	0	0	0
	[l/s] (CH4)	%	0	1147.73	0	0	0	0	0	0
	[l/s] (CO)	%	0	0	1147.73	0	0	0	0	0
	[l/s] (CO2)	%	0	0	0	1147.73	0	0	0	0
in_g_Nplus1 =	[torrl/s]	%	0	0	0	0	0	0	0	0

10.1.6. *Case 7) Multi-gas model.* Change ion induced gas desorption yields $\eta_{CO_2^+-H_2}$ and $\eta_{CO_2^+-CO_2}$. Comparison between Case 4 and 7

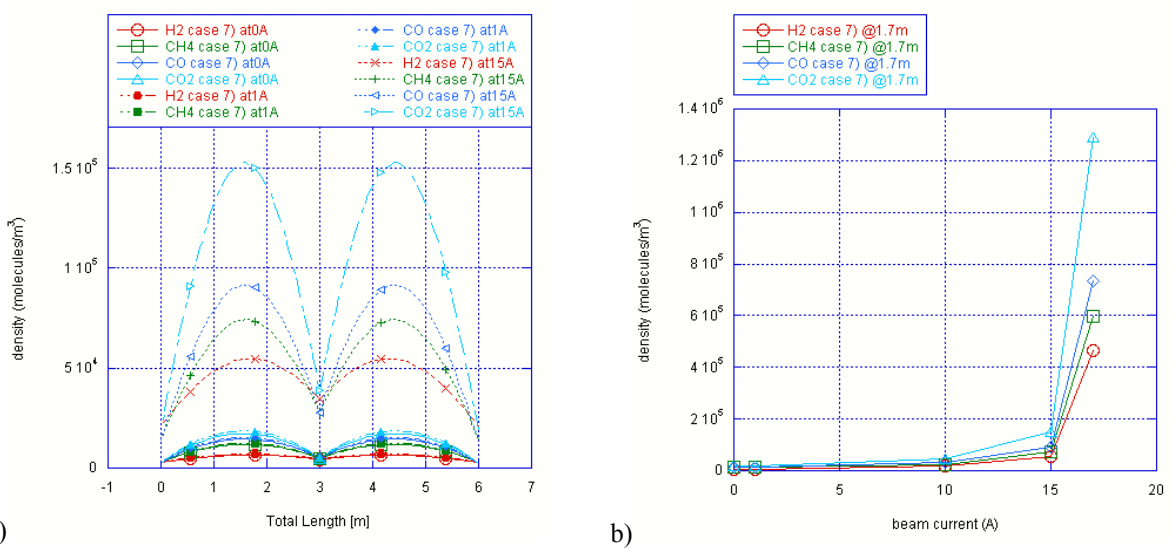

a) b)

Figure 12 a) Density profile at 10 and 15A beam current for Case 7 (Table 10); b) Density as a function of beam current for Case 7 at one location.

Observations:

- In Case 7, as before, the critical current is limited by CO_2. Therefore, the augmentation of the H_2 desorption yield induced by CO_2^+ does not affect very much the critical current. In *Figure 15* b) one can see that the H_2 density increases faster than both in Case 4 and Case 6, as it was to be expected. The densities of the other gas species are also affected, given the cross-correlation between different species, but in a much smaller proportion.

Table 10 - Case 7) Change ion induced gas desorption yields $\eta_{CO_2^+-H_2}$ *and* $\eta_{CO_2^+-CO_2} = 1$

%			H2	CH4	CO	CO2	H2	CH4	CO	CO2
in_Segment = [		%	1	0	0	0	2	0	0	0
in_d = [	[mm]	%	91.63	0	0	0	91.63	0	0	0
in_L = [	[mm]	%	3000	0	0	0	3000	0	0	0
in_dist_ref = [	[mm]	%	3000	0	0	0	6000	0	0	0
in_T = [	[K]	%	300	0	0	0	300	0	0	0
in_S = [	[l/s] (H2)	%	1147.73	0	0	0	548.35	0	0	0
	[l/s] (CH4)	%	0	1147.73	0	0	0	548.35	0	0
	[l/s] (CO)	%	0	0	1147.73	0	0	0	548.35	0
	[l/s] (CO2)	%	0	0	0	1147.73	0	0	0	548.35
in_g = [	[torrl/s]	%	0	0	0	0	0	0	0	0
in_sigma = [	[m2]	%	4.45E-23	0	0	0	4.45E-23	0	0	0
		%	0	3.18E-22	0	0	0	3.18E-22	0	0
		%	0	0	2.75E-22	0	0	0	2.75E-22	0
		%	0	0	0	4.29E-22	0	0	0	4.29E-22
in_alpha = [		%	0	0	0	0	0	0	0	0
		%	0	0	0	0	0	0	0	0
		%	0	0	0	0	0	0	0	0
		%	0	0	0	0	0	0	0	0
in_alpha_p = [		%	0	0	0	0	0	0	0	0
		%	0	0	0	0	0	0	0	0
		%	0	0	0	0	0	0	0	0
		%	0	0	0	0	0	0	0	0
in_eta_i = [		%	0.54	0.54	0.54	1	0.54	0.54	0.54	1
		%	0.54	0.54	0.54	0.54	0.54	0.54	0.54	0.54
		%	0.54	0.54	0.54	0.54	0.54	0.54	0.54	0.54
		%	0.54	0.54	0.54	1	0.54	0.54	0.54	1
in_eta_p_i = [		%	0	0	0	0	0	0	0	0
		%	0	0	0	0	0	0	0	0
		%	0	0	0	0	0	0	0	0
		%	0	0	0	0	0	0	0	0
in_eta_e = [		%	1.77E-03	1.77E-03	1.77E-03	1.77E-03	1.77E-03	1.77E-03	1.77E-03	1.77E-03
in_eta_p_e = [		%	0	0	0	0	0	0	0	0
in_eta_ph = [		%	1.50E-04	1.50E-04	1.50E-04	1.50E-04	1.50E-04	1.50E-04	1.50E-04	1.50E-04
in_eta_p_ph = [		%	0	0	0	0	0	0	0	0
in_Cbs = [	[l/s/m]	%	0	0	0	0	0	0	0	0
		%	0	0	0	0	0	0	0	0
		%	0	0	0	0	0	0	0	0
		%	0	0	0	0	0	0	0	0
in_Qth = [		%	1.00E-20	1.00E-20	1.00E-20	1.00E-20	1.00E-20	1.00E-20	1.00E-20	1.00E-20
in_n_e = [		%	0	0	0	0	0	0	0	0
in_N_e = [	[e-/m/s]	%	0	0	0	0	0	0	0	0
in_Gamma_ph	[ph/m/s]	%	0	0	0	0	0	0	0	0
in_S_Nplus1 =	[l/s] (H2)	%	1147.73	0	0	0	0	0	0	0
	[l/s] (CH4)	%	0	1147.73	0	0	0	0	0	0
	[l/s] (CO)	%	0	0	1147.73	0	0	0	0	0
	[l/s] (CO2)	%	0	0	0	1147.73	0	0	0	0
in_g_Nplus1 =	[torrl/s]	%	0	0	0	0	0	0	0	0

10.1.7. *Case 8) Multi-gas model.* Change ion induced gas desorption yields $\eta_{CO_2^+-CO_2}$, $\eta_{H_2^+-CO_2}$ and $\eta_{CO_2^+-H_2}$. Comparison between Case 4 and 8

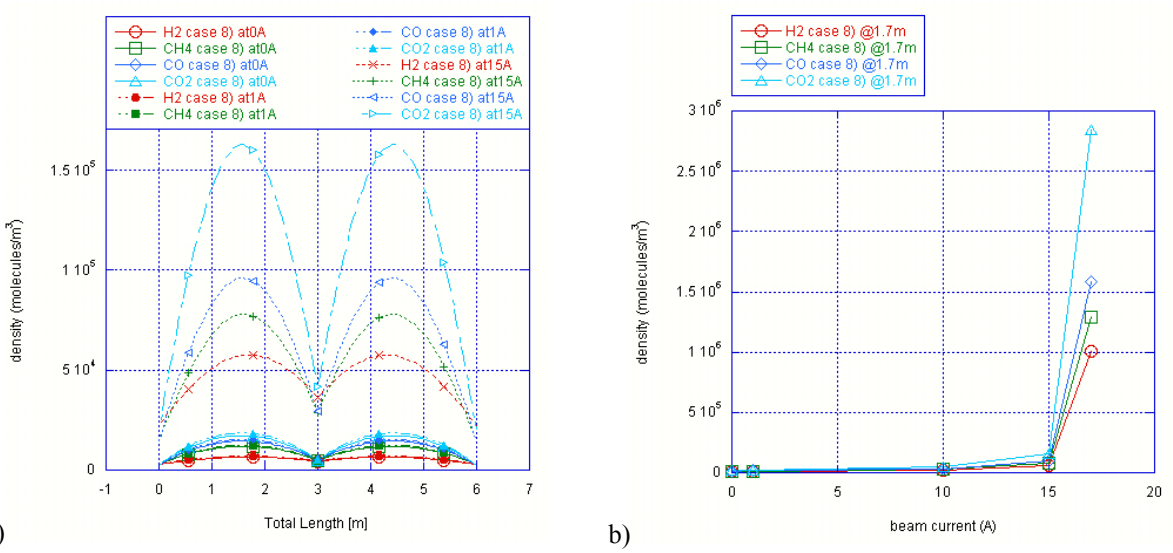

a) b)

Figure 13 a) Density profile at 10 and 15A beam current for Case 8 (Table 11); b) Density as a function of beam current for Case 8 at one location.

Observations:

- In Case 8, again, the critical current is limited by CO_2. The ratio between the critical current in Case 4) and Case 8) is about 1.25, while the ratio between the term determining the critical current: $\frac{I}{e}\cdot\left(\eta_{i,CO_2\to CO_2}\cdot\sigma_{CO_2}\cdot n_{CO_2}+\sum_{gas\neq CO_2}\{\eta_{i,gas-CO_2}\cdot\sigma_{gas}\cdot n_{gas}\}\right)$ in the two cases is about 1.45. This difference must be due to the different gas density.
- Comparing the evolution of the density with beam current (*Figure 15* c), one can see that all gas species are affected by the increment of $\eta_{CO_2^+-CO_2}$, since they all increase faster than in Case 4.

Table 11 - Case 8) Change ion induced gas desorption yields $\eta_{CO_2^+-CO_2}$, $\eta_{H_2^+-CO_2}$ *and* $\eta_{CO_2^+-H_2}=1$

%			H2	CH4	CO	CO2	H2	CH4	CO	CO2
in_Segment = [		%	1	0	0	0	2	0	0	0
in_d = [	[mm]	%	91.63	0	0	0	91.63	0	0	0
in_L = [	[mm]	%	3000	0	0	0	3000	0	0	0
in_dist_ref = [	[mm]	%	3000	0	0	0	6000	0	0	0
in_T = [	[K]	%	300	0	0	0	300	0	0	0
in_S = [	[l/s] (H2)	%	1147.73	0	0	0	548.35	0	0	0
	[l/s] (CH4)	%	0	1147.73	0	0	0	548.35	0	0
	[l/s] (CO)	%	0	0	1147.73	0	0	0	548.35	0
	[l/s] (CO2)	%	0	0	0	1147.73	0	0	0	548.35
in_g = [	[torrl/s]	%	0	0	0	0	0	0	0	0
in_sigma = [	[m2]	%	4.45E-23	0	0	0	4.45E-23	0	0	0
		%	0	3.18E-22	0	0	0	3.18E-22	0	0
		%	0	0	2.75E-22	0	0	0	2.75E-22	0
		%	0	0	0	4.29E-22	0	0	0	4.29E-22
in_alpha = [		%	0	0	0	0	0	0	0	0
		%	0	0	0	0	0	0	0	0
		%	0	0	0	0	0	0	0	0
		%	0	0	0	0	0	0	0	0
in_alpha_p = [		%	0	0	0	0	0	0	0	0
		%	0	0	0	0	0	0	0	0
		%	0	0	0	0	0	0	0	0
		%	0	0	0	0	0	0	0	0
in_eta_i = [		%	0.54	0.54	0.54	1	0.54	0.54	0.54	1
		%	0.54	0.54	0.54	0.54	0.54	0.54	0.54	0.54
		%	0.54	0.54	0.54	0.54	0.54	0.54	0.54	0.54
		%	1	0.54	0.54	1	1	0.54	0.54	1
in_eta_p_i = [		%	0	0	0	0	0	0	0	0
		%	0	0	0	0	0	0	0	0
		%	0	0	0	0	0	0	0	0
		%	0	0	0	0	0	0	0	0
in_eta_e = [		%	1.77E-03	1.77E-03	1.77E-03	1.77E-03	1.77E-03	1.77E-03	1.77E-03	1.77E-03
in_eta_p_e = [		%	0	0	0	0	0	0	0	0
in_eta_ph = [		%	1.50E-04	1.50E-04	1.50E-04	1.50E-04	1.50E-04	1.50E-04	1.50E-04	1.50E-04
in_eta_p_ph = [		%	0	0	0	0	0	0	0	0
in_Cbs = [	[l/s/m]	%	0	0	0	0	0	0	0	0
		%	0	0	0	0	0	0	0	0
		%	0	0	0	0	0	0	0	0
		%	0	0	0	0	0	0	0	0
in_Qth = [		%	1.00E-20	1.00E-20	1.00E-20	1.00E-20	1.00E-20	1.00E-20	1.00E-20	1.00E-20
in_n_e = [		%	0	0	0	0	0	0	0	0
in_N_e = [	[e-/m/s]	%	0	0	0	0	0	0	0	0
in_Gamma_ph	[ph/m/s]	%	0	0	0	0	0	0	0	0
in_S_Nplus1 =	[l/s] (H2)	%	1147.73	0	0	0	0	0	0	0
	[l/s] (CH4)	%	0	1147.73	0	0	0	0	0	0
	[l/s] (CO)	%	0	0	1147.73	0	0	0	0	0
	[l/s] (CO2)	%	0	0	0	1147.73	0	0	0	0
in_g_Nplus1 =	[torrl/s]	%	0	0	0	0	0	0	0	0

10.1.8. *Case 9) Multi-gas model.* Change ion induced gas desorption of molecules by CO_2^+ ions. Comparison between Case 4 and 9

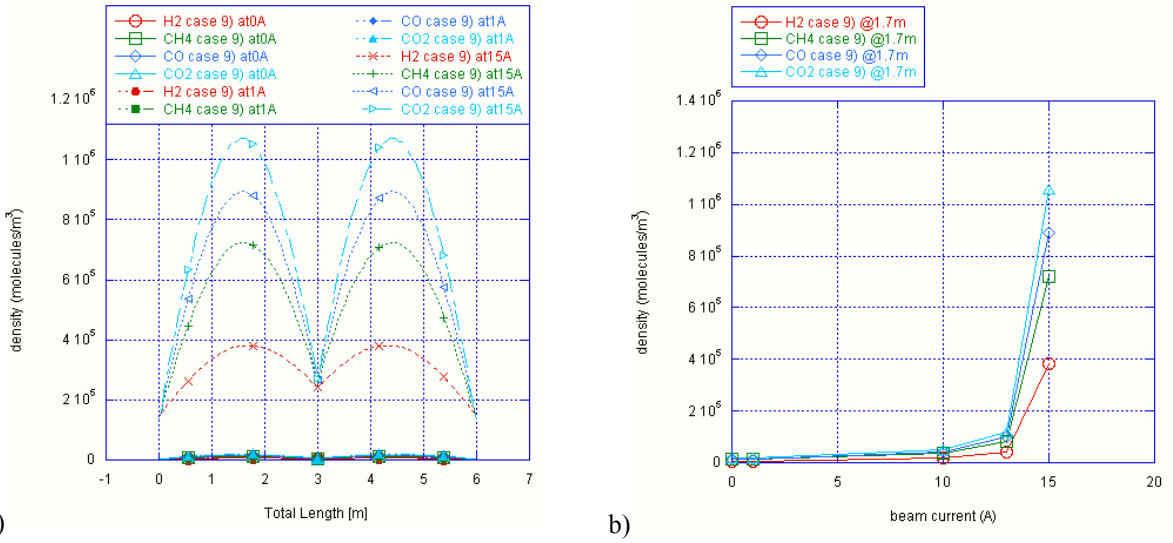

a) b)

Figure 14 a) Density profile at 10 and 15A beam current for Case 9 (Table 12); b) Density as a function of beam current for Case 9 at one location.

Observations:

– In Case 9, all gas species are desorbed by CO_2^+ ions at a faster rate with respect to before (see *Figure 15* d). The critical current is therefore lower.

Table 12 - Case 9) Change ion induced gas desorption yields in the 4th column (desoption of molecules by CO_2^+ ions)

%			H2	CH4	CO	CO2	H2	CH4	CO	CO2
in_Segment = [		%	1	0	0	0	2	0	0	0
in_d = [	[mm]	%	91.63	0	0	0	91.63	0	0	0
in_L = [	[mm]	%	3000	0	0	0	3000	0	0	0
in_dist_ref = [	[mm]	%	3000	0	0	0	6000	0	0	0
in_T = [	[K]	%	300	0	0	0	300	0	0	0
in_S = [	[l/s] (H2)	%	1147.73	0	0	0	548.35	0	0	0
	[l/s] (CH4)	%	0	1147.73	0	0	0	548.35	0	0
	[l/s] (CO)	%	0	0	1147.73	0	0	0	548.35	0
	[l/s] (CO2)	%	0	0	0	1147.73	0	0	0	548.35
in_g = [	[torrl/s]	%	0	0	0	0	0	0	0	0
in_sigma = [	[m2]	%	4.45E-23	0	0	0	4.45E-23	0	0	0
		%	0	3.18E-22	0	0	0	3.18E-22	0	0
		%	0	0	2.75E-22	0	0	0	2.75E-22	0
		%	0	0	0	4.29E-22	0	0	0	4.29E-22
in_alpha = [		%	0	0	0	0	0	0	0	0
		%	0	0	0	0	0	0	0	0
		%	0	0	0	0	0	0	0	0
		%	0	0	0	0	0	0	0	0
in_alpha_p = [		%	0	0	0	0	0	0	0	0
		%	0	0	0	0	0	0	0	0
		%	0	0	0	0	0	0	0	0
		%	0	0	0	0	0	0	0	0
in_eta_i = [		%	0.54	0.54	0.54	1	0.54	0.54	0.54	1
		%	0.54	0.54	0.54	1	0.54	0.54	0.54	1
		%	0.54	0.54	0.54	1	0.54	0.54	0.54	1
		%	0.54	0.54	0.54	1	0.54	0.54	0.54	1
in_eta_p_i = [		%	0	0	0	0	0	0	0	0
		%	0	0	0	0	0	0	0	0
		%	0	0	0	0	0	0	0	0
		%	0	0	0	0	0	0	0	0
in_eta_e = [		%	1.77E-03	1.77E-03	1.77E-03	1.77E-03	1.77E-03	1.77E-03	1.77E-03	1.77E-03
in_eta_p_e = [		%	0	0	0	0	0	0	0	0
in_eta_ph = [		%	1.50E-04	1.50E-04	1.50E-04	1.50E-04	1.50E-04	1.50E-04	1.50E-04	1.50E-04
in_eta_p_ph = [		%	0	0	0	0	0	0	0	0
in_Cbs = [	[l/s/m]	%	0	0	0	0	0	0	0	0
		%	0	0	0	0	0	0	0	0
		%	0	0	0	0	0	0	0	0
		%	0	0	0	0	0	0	0	0
in_Qth = [		%	1.00E-20	1.00E-20	1.00E-20	1.00E-20	1.00E-20	1.00E-20	1.00E-20	1.00E-20
in_n_e = [		%	0	0	0	0	0	0	0	0
in_N_e = [	[e-/m/s]	%	0	0	0	0	0	0	0	0
in_Gamma_ph	[ph/m/s]	%	0	0	0	0	0	0	0	0
in_S_Nplus1 =	[l/s] (H2)	%	1147.73	0	0	0	0	0	0	0
	[l/s] (CH4)	%	0	1147.73	0	0	0	0	0	0
	[l/s] (CO)	%	0	0	1147.73	0	0	0	0	0
	[l/s] (CO2)	%	0	0	0	1147.73	0	0	0	0
in_g_Nplus1 =	[torrl/s]	%	0	0	0	0	0	0	0	0

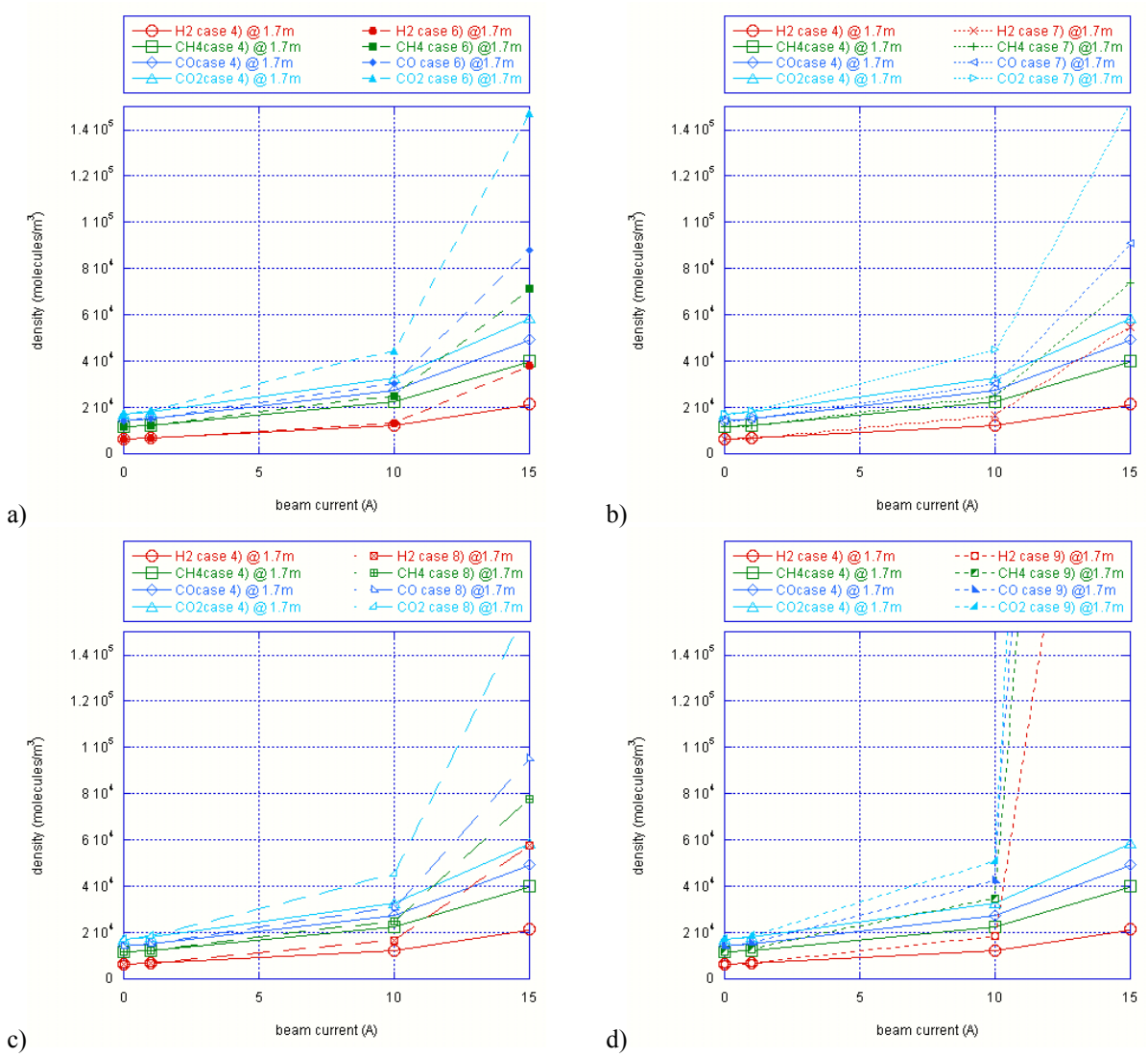

Figure 15 Density as a function of beam current at one location for a) Case 4 & 6; b) Case 4 & 7; c) Case 4 & 8; c) Case 4 & 9.

10.1.9. Multi-gas model. Ion induced desorption yields from a real case with comparison between Case 4 and 10

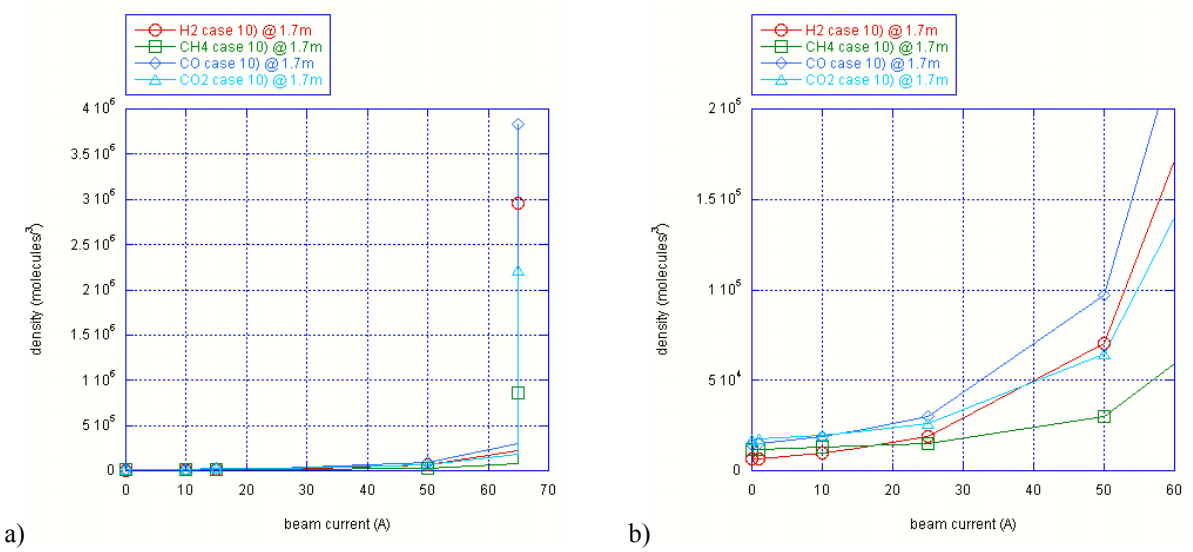

Figure 16 a) Density as a function of beam current for Case 10 (Table 13) at one location; b) Zoom in.

Observations:

– This case is very different from the previous ones, in that the ion induced desorption yields depend on gas species. The critical current is dominated by CO and no longer by CO_2. This is because the ratio $\frac{\frac{I}{e}\cdot\left(\eta_{i,CO^+\to CO}\cdot\sigma_{CO}\cdot n_{CO}+\sum_{gas\neq CO}\left\{\eta_{i,gas^+-CO}\cdot\sigma_{gas}\cdot n_{gas}\right\}\right)}{\frac{I}{e}\cdot\left(\eta_{i,CO_2^+\to CO_2}\cdot\sigma_{CO_2}\cdot n_{CO_2}+\sum_{gas\neq CO_2}\left\{\eta_{i,gas^+-CO_2}\cdot\sigma_{gas}\cdot n_{gas}\right\}\right)}$, is about 2.1 while between the relative conductances is only 1.25. The net production of CO (desorbed – pumped) is therefore faster than for CO_2. Note that hydrogen has the highest ion desorption yield (1st row) but also the highest pumping (a factor 3.74 higher than CO).

– Also the evolution of gas density as a function of beam current is different is this case. At zero current, the gas density is purely determined by the difference conductances (given that the thermal outgassing in this case is the same for all gas species). As the current is increased, the species with the highest desorption yields grow faster than the other, and CO dominates (see also *Figure 17*).

Table 13 - Case 10) Ion induced gas desorption yields as estimated in a real case for ion impact energy of 300eV

%			H2	CH4	CO	CO2	H2	CH4	CO	CO2
in_Segment = [		%	1	0	0	0	2	0	0	0
in_d = [	[mm]	%	91.63	0	0	0	91.63	0	0	0
in_L = [	[mm]	%	3000	0	0	0	3000	0	0	0
in_dist_ref = [	[mm]	%	3000	0	0	0	6000	0	0	0
in_T = [	[K]	%	300	0	0	0	300	0	0	0
in_S = [	[l/s] (H2)	%	1147.73	0	0	0	548.35	0	0	0
	[l/s] (CH4)	%	0	1147.73	0	0	0	548.35	0	0
	[l/s] (CO)	%	0	0	1147.73	0	0	0	548.35	0
	[l/s] (CO2)	%	0	0	0	1147.73	0	0	0	548.35
in_g = [	[torrl/s]	%	0	0	0	0	0	0	0	0
in_sigma = [	[m2]	%	4.45E-23	0	0	0	4.45E-23	0	0	0
		%	0	3.18E-22	0	0	0	3.18E-22	0	0
		%	0	0	2.75E-22	0	0	0	2.75E-22	0
		%	0	0	0	4.29E-22	0	0	0	4.29E-22
in_alpha = [		%	0	0	0	0	0	0	0	0
		%	0	0	0	0	0	0	0	0
		%	0	0	0	0	0	0	0	0
		%	0	0	0	0	0	0	0	0
in_alpha_p = [		%	0	0	0	0	0	0	0	0
		%	0	0	0	0	0	0	0	0
		%	0	0	0	0	0	0	0	0
		%	0	0	0	0	0	0	0	0
in_eta_i = [		%	0.54	0.54	0.54	0.54	0.54	0.54	0.54	0.54
		%	0.04	0.05	0.07	0.11	0.04	0.05	0.07	0.11
		%	0.25	0.29	0.29	0.33	0.25	0.29	0.29	0.33
		%	0.14	0.14	0.14	0.14	0.14	0.14	0.14	0.14
in_eta_p_i = [		%	0	0	0	0	0	0	0	0
		%	0	0	0	0	0	0	0	0
		%	0	0	0	0	0	0	0	0
		%	0	0	0	0	0	0	0	0
in_eta_e = [		%	1.77E-03	1.77E-03	1.77E-03	1.77E-03	1.77E-03	1.77E-03	1.77E-03	1.77E-03
in_eta_p_e = [		%	0	0	0	0	0	0	0	0
in_eta_ph = [		%	1.50E-04	1.50E-04	1.50E-04	1.50E-04	1.50E-04	1.50E-04	1.50E-04	1.50E-04
in_eta_p_ph = [		%	0	0	0	0	0	0	0	0
in_Cbs = [	[l/s/m]	%	0	0	0	0	0	0	0	0
		%	0	0	0	0	0	0	0	0
		%	0	0	0	0	0	0	0	0
		%	0	0	0	0	0	0	0	0
in_Qth = [		%	1.00E-20	1.00E-20	1.00E-20	1.00E-20	1.00E-20	1.00E-20	1.00E-20	1.00E-20
in_n_e = [		%	0	0	0	0	0	0	0	0
in_N_e = [	[e-/m/s]	%	0	0	0	0	0	0	0	0
in_Gamma_ph	[ph/m/s]	%	0	0	0	0	0	0	0	0
in_S_Nplus1 =	[l/s] (H2)	%	1147.73	0	0	0	0	0	0	0
	[l/s] (CH4)	%	0	1147.73	0	0	0	0	0	0
	[l/s] (CO)	%	0	0	1147.73	0	0	0	0	0
	[l/s] (CO2)	%	0	0	0	1147.73	0	0	0	0
in_g_Nplus1 =	[torrl/s]	%	0	0	0	0	0	0	0	0

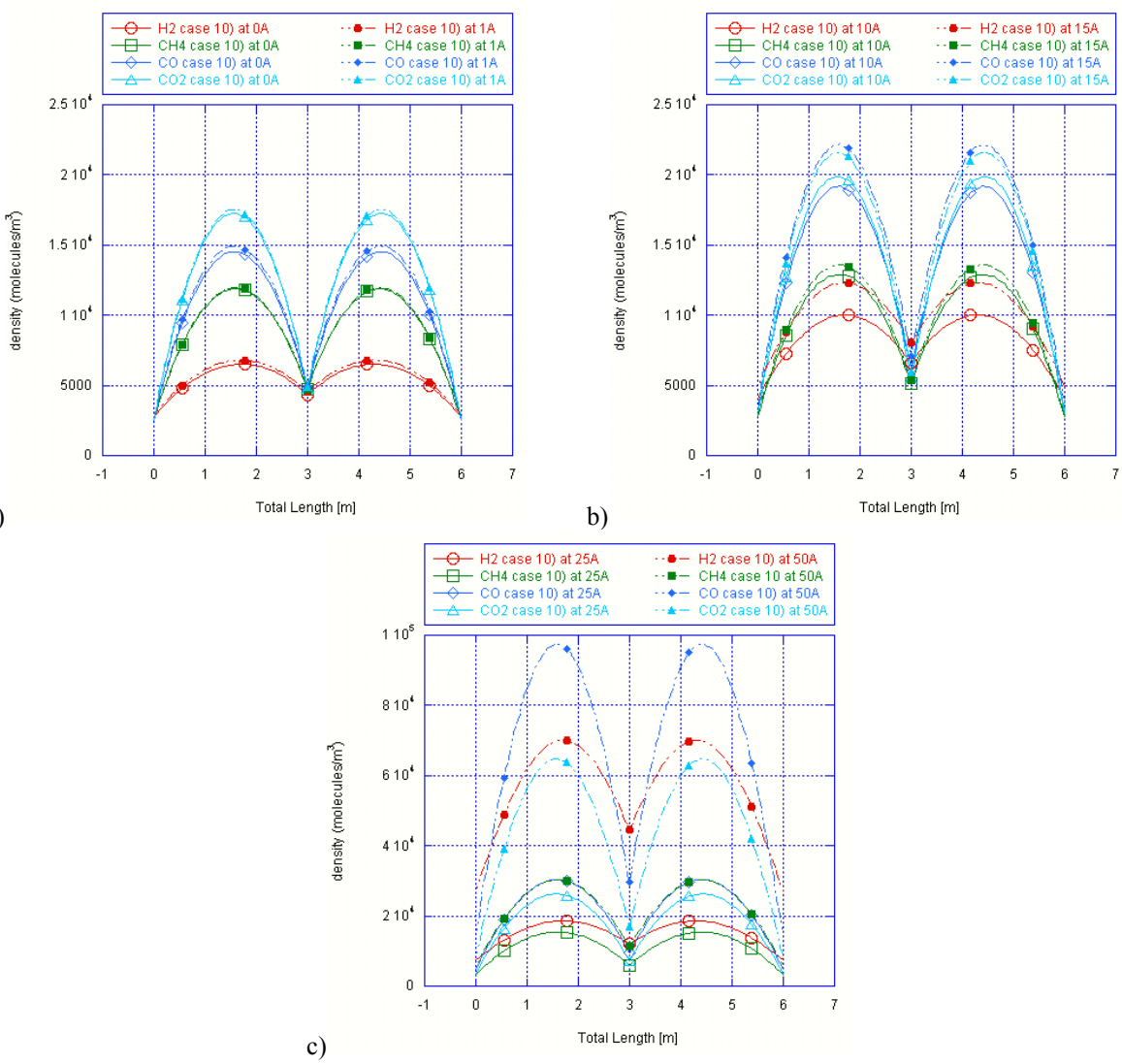

Figure 17 Density profile for Case 10 at a) 0 and 1A beam current; b) 10 and 15A beam current; c) 25 and 50A beam current.

10.2. Variation of the sources independent of gas density

In this section the variation of gas sources independent of gas density, i.e. variation to the input parameters composing the matrix $\overline{C}$ (equation (24)) is analysed both for the "single-gas" and the "multi-gas" models. As it is shown in Table 3, the critical current is independent of these sources, since they do not contribute to the amplification process.

10.2.1. *Case 11) Single-gas model.* Add sources independent of gas density to Case 2

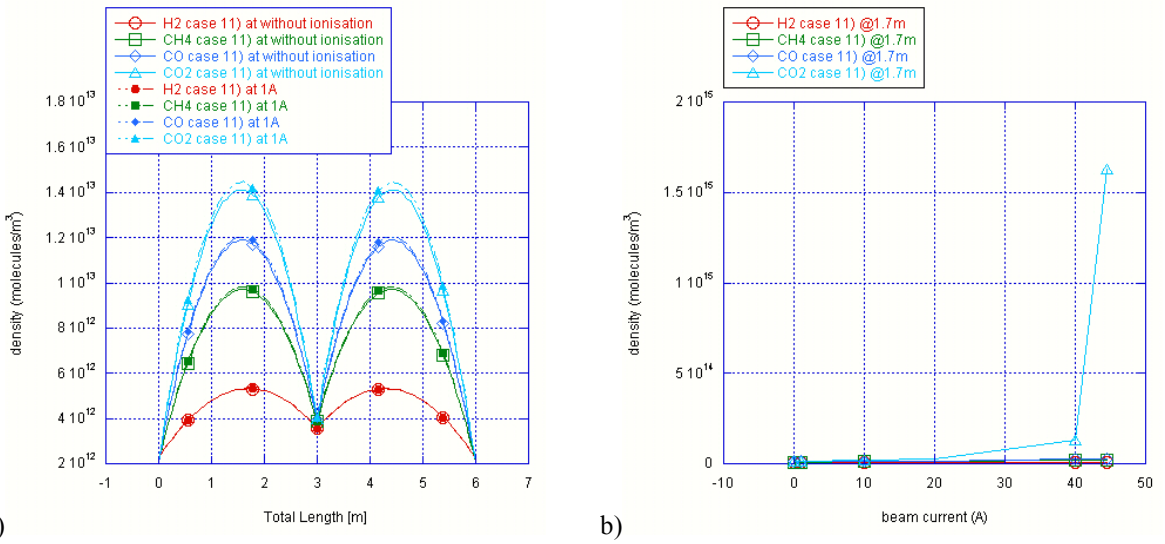

Figure 18 a) Density profile without contribution of ion induced desorption and with contribution at 1A beam current for Case 11 (Table 14); b) Density as a function of beam current for Case 11 at one location.

Table 14 - Case 11) Add sources independent of gas density to Case 2

%			H2	CH4	CO	CO2	H2	CH4	CO	CO2
in_Segment = [		%	1	0	0	0	2	0	0	0
in_d = [	[mm]	%	91.63	0	0	0	91.63	0	0	0
in_L = [	[mm]	%	3000	0	0	0	3000	0	0	0
in_dist_ref = [	[mm]	%	3000	0	0	0	6000	0	0	0
in_T = [	[K]	%	300	0	0	0	300	0	0	0
in_S = [	[l/s] (H2)	%	1147.73	0	0	0	548.35	0	0	0
	[l/s] (CH4)	%	0	1147.73	0	0	0	548.35	0	0
	[l/s] (CO)	%	0	0	1147.73	0	0	0	548.35	0
	[l/s] (CO2)	%	0	0	0	1147.73	0	0	0	548.35
in_g = [	[torrl/s]	%	0	0	0	0	0	0	0	0
in_sigma = [	[m2]	%	4.45E-23	0	0	0	4.45E-23	0	0	0
		%	0	3.18E-22	0	0	0	3.18E-22	0	0
		%	0	0	2.75E-22	0	0	0	2.75E-22	0
		%	0	0	0	4.29E-22	0	0	0	4.29E-22
in_alpha = [		%	0	0	0	0	0	0	0	0
		%	0	0	0	0	0	0	0	0
		%	0	0	0	0	0	0	0	0
		%	0	0	0	0	0	0	0	0
in_alpha_p = [		%	0	0	0	0	0	0	0	0
		%	0	0	0	0	0	0	0	0
		%	0	0	0	0	0	0	0	0
		%	0	0	0	0	0	0	0	0
in_eta_i = [		%	0.54	0	0	0	0.54	0	0	0
		%	0	0.54	0	0	0	0.54	0	0
		%	0	0	0.54	0	0	0	0.54	0
		%	0	0	0	0.54	0	0	0	0.54
in_eta_p_i = [		%	0	0	0	0	0	0	0	0
		%	0	0	0	0	0	0	0	0
		%	0	0	0	0	0	0	0	0
		%	0	0	0	0	0	0	0	0
in_eta_e = [		%	1.77E-03	1.77E-03	1.77E-03	1.77E-03	1.77E-03	1.77E-03	1.77E-03	1.77E-03
in_eta_p_e = [		%	0	0	0	0	0	0	0	0
in_eta_ph = [		%	1.50E-04	1.50E-04	1.50E-04	1.50E-04	1.50E-04	1.50E-04	1.50E-04	1.50E-04
in_eta_p_ph = [		%	0	0	0	0	0	0	0	0
in_Cbs = [	[l/s/m]	%	0	0	0	0	0	0	0	0
		%	0	0	0	0	0	0	0	0
		%	0	0	0	0	0	0	0	0
		%	0	0	0	0	0	0	0	0
in_Qth = [		%	1.00E-12	1.00E-12	1.00E-12	1.00E-12	1.00E-12	1.00E-12	1.00E-12	1.00E-12
in_n_e = [		%	0	0	0	0	0	0	0	0
in_N_e = [	[e-/m/s]	%	1.2E+14	0	0	0	1.2E+14	0	0	0
in_Gamma_ph	[ph/m/s]	%	3E+15	0	0	0	3E+15	0	0	0
in_S_Nplus1 =	[l/s] (H2)	%	1147.73	0	0	0	0	0	0	0
	[l/s] (CH4)	%	0	1147.73	0	0	0	0	0	0
	[l/s] (CO)	%	0	0	1147.73	0	0	0	0	0
	[l/s] (CO2)	%	0	0	0	1147.73	0	0	0	0
in_g_Nplus1 =	[torrl/s]	%	0	0	0	0	0	0	0	0

Observations:

- The overall density profile in Case 11 is of course much higher than in Case 2, due to the additional gas sources.

– The critical current on the other hand is not affected by these sources, as expected, since they do not contribute to the "gain" of the avalanche effect.

10.2.2. *Case 12) Multi-gas model against Single-gas model.*) Add sources independent of gas density to Case 4

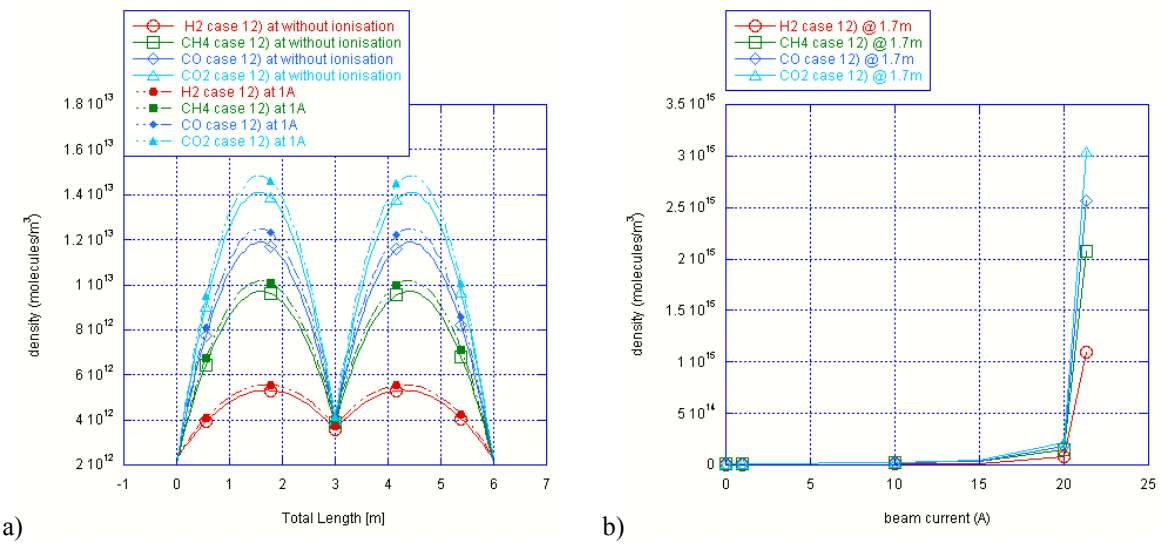

a) b)

Figure 19 a) Density profile without contribution of ion induced desorption and with contribution at 1A beam current for Case 12 (Table 15); b) Density as a function of beam current for Case 12 at one location.

Observations:

The same considerations as in Case 11 hold:

– The overall density profile in Case 12 is of course much higher than in Case 4, due to the additional gas sources.

– The critical current is not affected by these sources, as expected, since they do not contribute to the "gain" of the avalanche effect.

Table 15 - Case 12) Add sources independent of gas density to Case 4

%			H2	CH4	CO	CO2	H2	CH4	CO	CO2
in_Segment = [		%	1	0	0	0	2	0	0	0
in_d = [	[mm]	%	91.63	0	0	0	91.63	0	0	0
in_L = [	[mm]	%	3000	0	0	0	3000	0	0	0
in_dist_ref = [	[mm]	%	3000	0	0	0	6000	0	0	0
in_T = [	[K]	%	300	0	0	0	300	0	0	0
in_S = [	[l/s] (H2)	%	1147.73	0	0	0	548.35	0	0	0
	[l/s] (CH4)	%	0	1147.73	0	0	0	548.35	0	0
	[l/s] (CO)	%	0	0	1147.73	0	0	0	548.35	0
	[l/s] (CO2)	%	0	0	0	1147.73	0	0	0	548.35
in_g = [	[torrl/s]	%	0	0	0	0	0	0	0	0
in_sigma = [	[m2]	%	4.45E-23	0	0	0	4.45E-23	0	0	0
		%	0	3.18E-22	0	0	0	3.18E-22	0	0
		%	0	0	2.75E-22	0	0	0	2.75E-22	0
		%	0	0	0	4.29E-22	0	0	0	4.29E-22
in_alpha = [		%	0	0	0	0	0	0	0	0
		%	0	0	0	0	0	0	0	0
		%	0	0	0	0	0	0	0	0
		%	0	0	0	0	0	0	0	0
in_alpha_p = [		%	0	0	0	0	0	0	0	0
		%	0	0	0	0	0	0	0	0
		%	0	0	0	0	0	0	0	0
		%	0	0	0	0	0	0	0	0
in_eta_i = [		%	0.54	0.54	0.54	0.54	0.54	0.54	0.54	0.54
		%	0.54	0.54	0.54	0.54	0.54	0.54	0.54	0.54
		%	0.54	0.54	0.54	0.54	0.54	0.54	0.54	0.54
		%	0.54	0.54	0.54	0.54	0.54	0.54	0.54	0.54
in_eta_p_i = [		%	0	0	0	0	0	0	0	0
		%	0	0	0	0	0	0	0	0
		%	0	0	0	0	0	0	0	0
		%	0	0	0	0	0	0	0	0
in_eta_e = [		%	1.77E-03	1.77E-03	1.77E-03	1.77E-03	1.77E-03	1.77E-03	1.77E-03	1.77E-03
in_eta_p_e = [		%	0	0	0	0	0	0	0	0
in_eta_ph = [		%	1.50E-04	1.50E-04	1.50E-04	1.50E-04	1.50E-04	1.50E-04	1.50E-04	1.50E-04
in_eta_p_ph = [		%	0	0	0	0	0	0	0	0
in_Cbs = [	[l/s/m]	%	0	0	0	0	0	0	0	0
		%	0	0	0	0	0	0	0	0
		%	0	0	0	0	0	0	0	0
		%	0	0	0	0	0	0	0	0
in_Qth = [		%	1.00E-12	1.00E-12	1.00E-12	1.00E-12	1.00E-12	1.00E-12	1.00E-12	1.00E-12
in_n_e = [		%	0	0	0	0	0	0	0	0
in_N_e = [	[e-/m/s]	%	1.2E+14	0	0	0	1.2E+14	0	0	0
in_Gamma_ph	[ph/m/s]	%	3E+15	0	0	0	3E+15	0	0	0
in_S_Nplus1 =	[l/s] (H2)	%	1147.73	0	0	0	0	0	0	0
	[l/s] (CH4)	%	0	1147.73	0	0	0	0	0	0
	[l/s] (CO)	%	0	0	1147.73	0	0	0	0	0
	[l/s] (CO2)	%	0	0	0	1147.73	0	0	0	0
in_g_Nplus1 =	[torrl/s]	%	0	0	0	0	0	0	0	0

10.2.3. *Case 13) Multi-gas model.* Reduce sources independent of gas density by 1/100 with respect to Case 13)

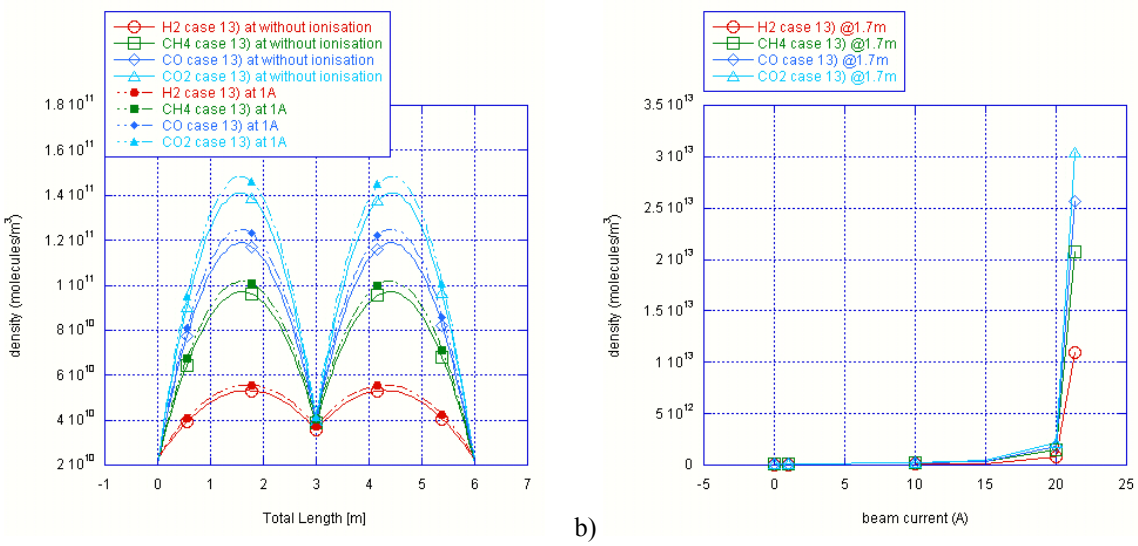

a) b)

Figure 20 a) Density profile without contribution of ion induced desorption and with contribution at 1A beam current for Case 13 (Table 16); b) Density as a function of beam current for Case 13 at one location.

Observations:

- The critical current is not affected by the reduction of sources independent of gas density, and is the same in the two cases 12 and 13.
- The ratio between the gas density in Case 12 and Case 13 equals the ratio between these sources.

Table 16 - Case 13) reduce sources independent of gas density by 1/100 with respect to Case 12)

%			H2	CH4	CO	CO2	H2	CH4	CO	CO2
in_Segment = [		%	1	0	0	0	2	0	0	0
in_d = [	[mm]	%	91.63	0	0	0	91.63	0	0	0
in_L = [	[mm]	%	3000	0	0	0	3000	0	0	0
in_dist_ref = [	[mm]	%	3000	0	0	0	6000	0	0	0
in_T = [	[K]	%	300	0	0	0	300	0	0	0
in_S = [	[l/s] (H2)	%	1147.73	0	0	0	548.35	0	0	0
	[l/s] (CH4)	%	0	1147.73	0	0	0	548.35	0	0
	[l/s] (CO)	%	0	0	1147.73	0	0	0	548.35	0
	[l/s] (CO2)	%	0	0	0	1147.73	0	0	0	548.35
in_g = [	[torrl/s]	%	0	0	0	0	0	0	0	0
in_sigma = [	[m2]	%	4.45E-23	0	0	0	4.45E-23	0	0	0
		%	0	3.18E-22	0	0	0	3.18E-22	0	0
		%	0	0	2.75E-22	0	0	0	2.75E-22	0
		%	0	0	0	4.29E-22	0	0	0	4.29E-22
in_alpha = [		%	0	0	0	0	0	0	0	0
		%	0	0	0	0	0	0	0	0
		%	0	0	0	0	0	0	0	0
		%	0	0	0	0	0	0	0	0
in_alpha_p = [		%	0	0	0	0	0	0	0	0
		%	0	0	0	0	0	0	0	0
		%	0	0	0	0	0	0	0	0
		%	0	0	0	0	0	0	0	0
in_eta_i = [		%	0.54	0.54	0.54	0.54	0.54	0.54	0.54	0.54
		%	0.54	0.54	0.54	0.54	0.54	0.54	0.54	0.54
		%	0.54	0.54	0.54	0.54	0.54	0.54	0.54	0.54
		%	0.54	0.54	0.54	0.54	0.54	0.54	0.54	0.54
in_eta_p_i = [		%	0	0	0	0	0	0	0	0
		%	0	0	0	0	0	0	0	0
		%	0	0	0	0	0	0	0	0
		%	0	0	0	0	0	0	0	0
in_eta_e = [		%	1.77E-03	1.77E-03	1.77E-03	1.77E-03	1.77E-03	1.77E-03	1.77E-03	1.77E-03
in_eta_p_e = [		%	0	0	0	0	0	0	0	0
in_eta_ph = [		%	1.50E-04	1.50E-04	1.50E-04	1.50E-04	1.50E-04	1.50E-04	1.50E-04	1.50E-04
in_eta_p_ph = [		%	0	0	0	0	0	0	0	0
in_Cbs = [	[l/s/m]	%	0	0	0	0	0	0	0	0
		%	0	0	0	0	0	0	0	0
		%	0	0	0	0	0	0	0	0
		%	0	0	0	0	0	0	0	0
in_Qth = [		%	1.00E-14	1.00E-14	1.00E-14	1.00E-14	1.00E-14	1.00E-14	1.00E-14	1.00E-14
in_n_e = [		%	0	0	0	0	0	0	0	0
in_N_e = [	[e-/m/s]	%	1.2E+12	0	0	0	1.2E+12	0	0	0
in_Gamma_ph	[ph/m/s]	%	3E+13	0	0	0	3E+13	0	0	0
in_S_Nplus1 =	[l/s] (H2)	%	1147.73	0	0	0	0	0	0	0
	[l/s] (CH4)	%	0	1147.73	0	0	0	0	0	0
	[l/s] (CO)	%	0	0	1147.73	0	0	0	0	0
	[l/s] (CO2)	%	0	0	0	1147.73	0	0	0	0
in_g_Nplus1 =	[torrl/s]	%	0	0	0	0	0	0	0	0

11. Multi-gas model. Real cases

In this section we present the evolution of gas density with beam current calculated with the parameters estimated from lab measurements. These parameters have been discussed in detailed in [4]. All desorption related parameters (induced desorption yields and thermal outgassing) depend on the gas species.
The variation of ion induced desorption yield values is again analysed. Two cases are studies:

- Case 14) All input parameters are selected as in [4]. In particular, the ion induced desorption yields were taken from measurements on baked Cu samples performed in [5] as a function of the incident ion at 5keV ion incident energy. These values were scaled at 300eV (ion energy as estimated in field free regions of the LHC Long Straight Section [6]) using the scaling factor from [7].
- Case 15) The ion induced desorption yields for Stainless Steel with $^{15}N_2^+$ incident ions from [7] are scaled with incident mass as from [8].

11.1. *Case 14) Multi-gas model, real case*

Observations:

- Case 10 and 14 have the same ion induce desorption yields values, and differ in the sources independent of gas density. As expected the critical current is the same in both cases, since it depends only on ion induce desorption yields and effective pumping speed (which includes the pumping and the conductances).
- In Case 14, the hydrogen thermal outgassing and the hydrogen contributions from photon and electron desorption are much higher than for the other gas species. Thus H_2 density at current =0, i.e. without ionisation, is the highest. As the current is increased, however, the net production of CO increases faster, given the higher ion induced desorption yield and the lower conductance. When the critical current is approached, CO species dominates the residual gas composition (see *Figure 21* and *Figure 22*) and determines the critical current.
- The evolution of the density with beam current (*Figure 21*) reproduces what observed in the Ion Storage Ring (ISR) when pressure runaway occurred [9].

Table 17 - Case 14) Replace parameters relative to desorption and thermal outgassing with measured values

%			H2	CH4	CO	CO2	H2	CH4	CO	CO2
in_Segment = [		%	1	0	0	0	2	0	0	0
in_d = [	[mm]	%	91.63	0	0	0	91.63	0	0	0
in_L = [	[mm]	%	3000	0	0	0	3000	0	0	0
in_dist_ref = [	[mm]	%	3000	0	0	0	6000	0	0	0
in_T = [	[K]	%	300	0	0	0	300	0	0	0
in_S = [	[l/s] (H2)	%	1147.73	0	0	0	548.35	0	0	0
	[l/s] (CH4)	%	0	1147.73	0	0	0	548.35	0	0
	[l/s] (CO)	%	0	0	1147.73	0	0	0	548.35	0
	[l/s] (CO2)	%	0	0	0	1147.73	0	0	0	548.35
in_g = [	[torrl/s]	%	0	0	0	0	0	0	0	0
in_sigma = [	[m2]	%	4.45E-23	0	0	0	4.45E-23	0	0	0
		%	0	3.18E-22	0	0	0	3.18E-22	0	0
		%	0	0	2.75E-22	0	0	0	2.75E-22	0
		%	0	0	0	4.29E-22	0	0	0	4.29E-22
in_alpha = [		%	0	0	0	0	0	0	0	0
		%	0	0	0	0	0	0	0	0
		%	0	0	0	0	0	0	0	0
		%	0	0	0	0	0	0	0	0
in_alpha_p = [		%	0	0	0	0	0	0	0	0
		%	0	0	0	0	0	0	0	0
		%	0	0	0	0	0	0	0	0
		%	0	0	0	0	0	0	0	0
in_eta_i = [		%	0.54	0.54	0.54	0.54	0.54	0.54	0.54	0.54
		%	0.04	0.05	0.07	0.11	0.04	0.05	0.07	0.11
		%	0.25	0.29	0.29	0.33	0.25	0.29	0.29	0.33
		%	0.14	0.14	0.14	0.14	0.14	0.14	0.14	0.14
in_eta_p_i = [		%	0	0	0	0	0	0	0	0
		%	0	0	0	0	0	0	0	0
		%	0	0	0	0	0	0	0	0
		%	0	0	0	0	0	0	0	0
in_eta_e = [		%	1.77E-03	6.46E-05	4.52E-04	3.87E-04	1.77E-03	6.46E-05	4.52E-04	3.87E-04
in_eta_p_e = [		%	0	0	0	0	0	0	0	0
in_eta_ph = [		%	1.50E-04	4.00E-06	1.50E-05	2.50E-05	1.50E-04	4.00E-06	1.50E-05	2.50E-05
in_eta_p_ph = [		%	0	0	0	0	0	0	0	0
in_Cbs = [	[l/s/m]	%	0	0	0	0	0	0	0	0
		%	0	0	0	0	0	0	0	0
		%	0	0	0	0	0	0	0	0
		%	0	0	0	0	0	0	0	0
in_Qth = [		%	1.00E-12	5.00E-15	1.00E-14	5.00E-15	1.00E-12	5.00E-15	1.00E-14	5.00E-15
in_n_e = [		%	0	0	0	0	0	0	0	0
in_N_e = [	[e-/m/s]	%	1.2E+14	0	0	0	1.2E+14	0	0	0
in_Gamma_ph	[ph/m/s]	%	3E+15	0	0	0	3E+15	0	0	0
in_S_Nplus1 =	[l/s] (H2)	%	1147.73	0	0	0	0	0	0	0
	[l/s] (CH4)	%	0	1147.73	0	0	0	0	0	0
	[l/s] (CO)	%	0	0	1147.73	0	0	0	0	0
	[l/s] (CO2)	%	0	0	0	1147.73	0	0	0	0
in_g_Nplus1 =	[torrl/s]	%	0	0	0	0	0	0	0	0

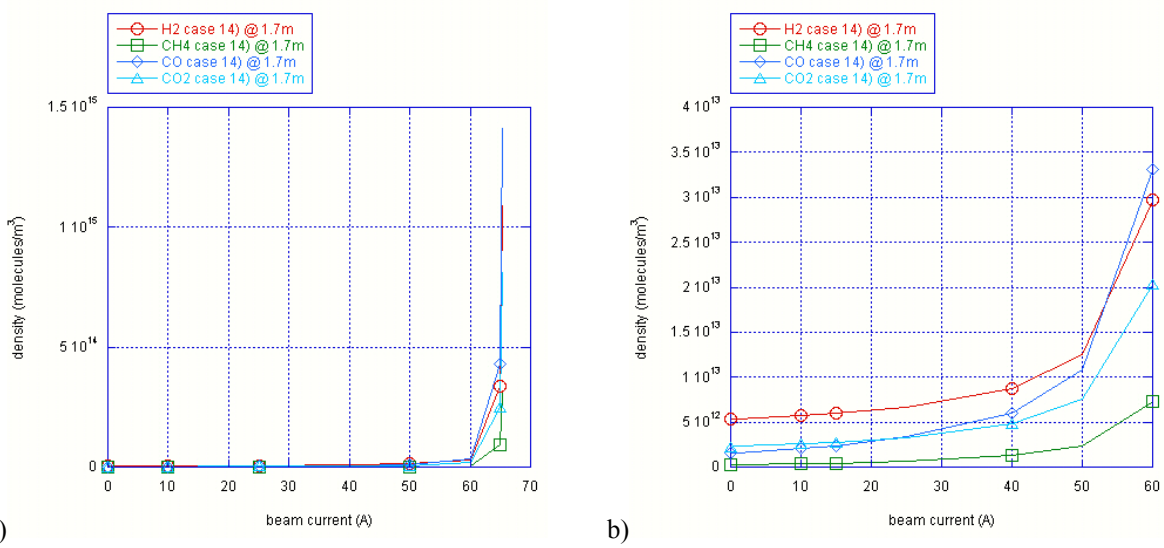

Figure 21 a) Density as a function of beam current for Case 14 (Table 17) at one location; b) Zoom in.

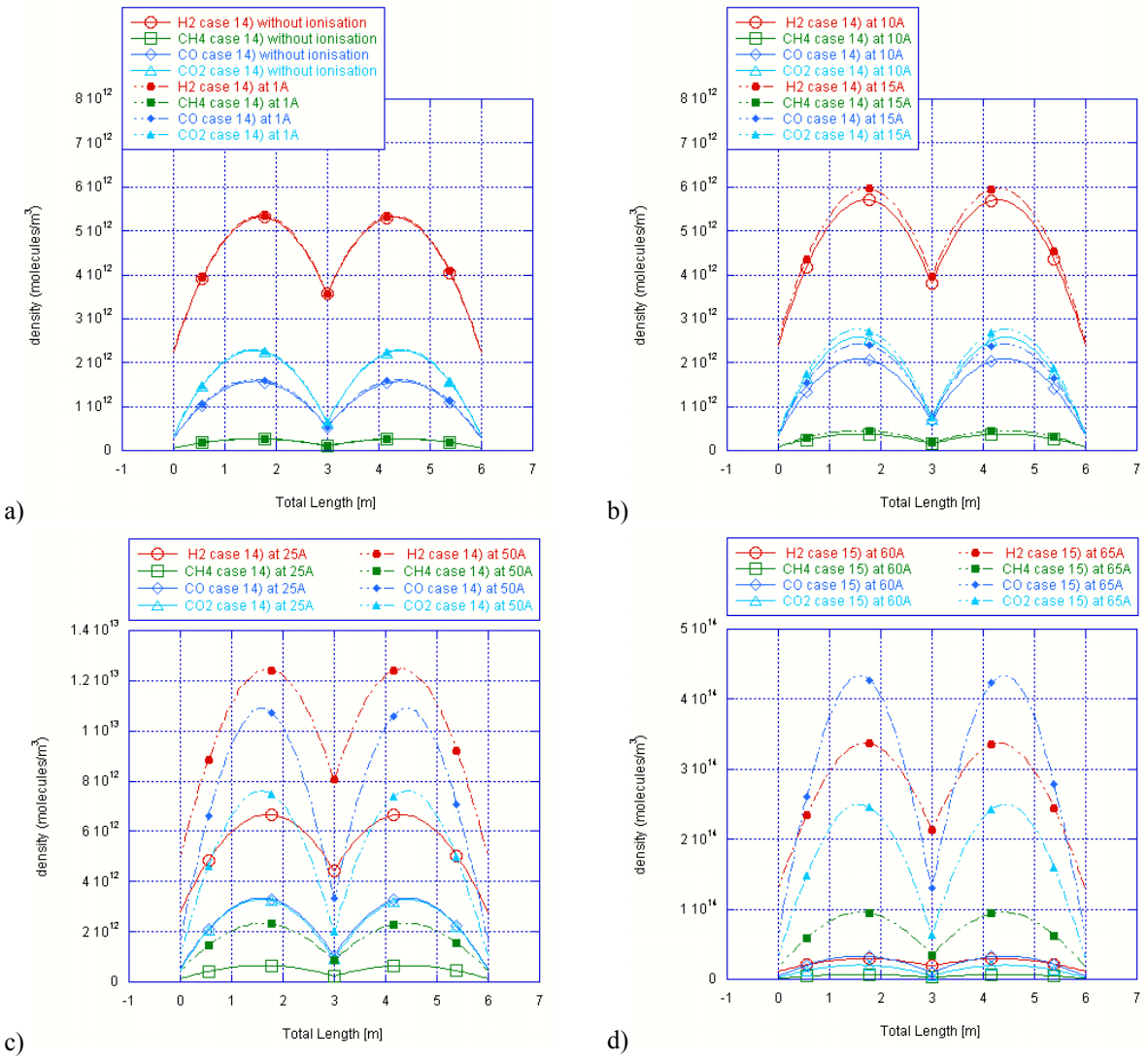

Figure 22 Density profile for Case 14 at a) 0 and 1A beam current; b) 10 and 15A beam current; c) 25 and 50A beam current; d) 60 and 65A beam current. Note that the vertical scale changes from figure to figure.

11.2. *Case 15) Multi-gas model, real case.* Change ion desorption yields with respect to case 14

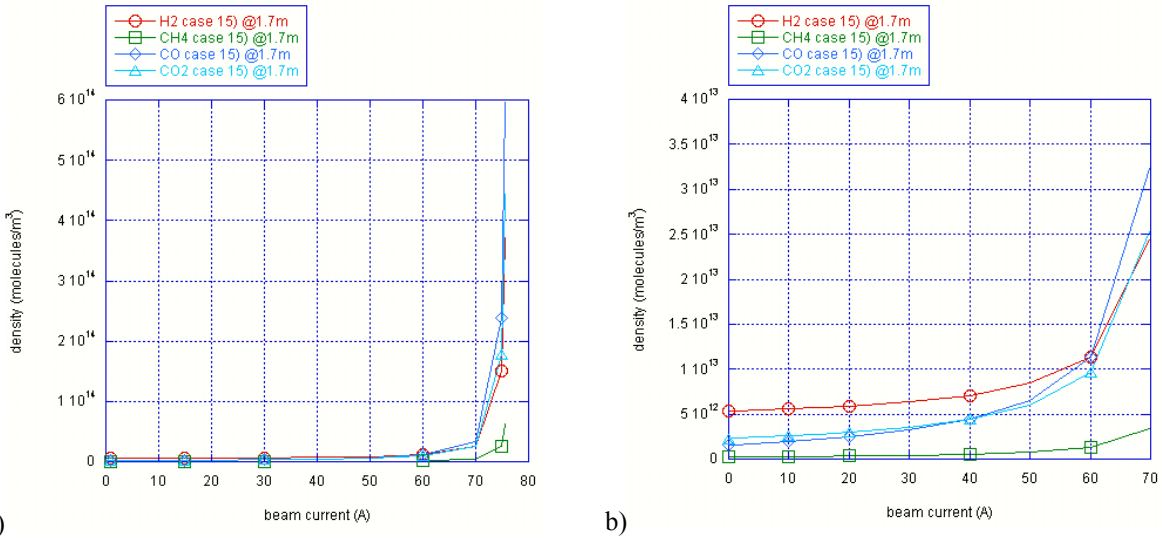

Figure 23 a) Density as a function of beam current for Case 15 (Table 18) at one location; b) Zoom in.

Observations:

- In Case 15, the dependence of ion induce desorption yields on the ion mass is more pronounced than in Case 14. On the other hand, the values are a bit larger in the latter case, for which the critical current is lower.
- In both cases the residual gas density is initially dominated by hydrogen (as explained before). As in Case 14, also in Case 15 the current is increased, the gas composition changes and CO becomes the main gas species (see *Figure 23* and *Figure 24*). The difference between the two cases is that for Case 14 the main gas is CO, followed by H_2, while in Case 15, CO_2 increases faster than H_2, and the gas abundance become comparable as approaching the critical current.

Table 18 - Case 15) Change ion desorption yields with respect to case 14

%			H2	CH4	CO	CO2	H2	CH4	CO	CO2
in_Segment = [		%	1	0	0	0	2	0	0	0
in_d = [	[mm]	%	91.63	0	0	0	91.63	0	0	0
in_L = [	[mm]	%	3000	0	0	0	3000	0	0	0
in_dist_ref = [	[mm]	%	3000	0	0	0	6000	0	0	0
in_T = [	[K]	%	300	0	0	0	300	0	0	0
in_S = [	[l/s] (H2)	%	1147.73	0	0	0	548.35	0	0	0
	[l/s] (CH4)	%	0	1147.73	0	0	0	548.35	0	0
	[l/s] (CO)	%	0	0	1147.73	0	0	0	548.35	0
	[l/s] (CO2)	%	0	0	0	1147.73	0	0	0	548.35
in_g = [	[torrl/s]	%	0	0	0	0	0	0	0	0
in_sigma = [	[m2]	%	4.45E-23	0	0	0	4.45E-23	0	0	0
		%	0	3.18E-22	0	0	0	3.18E-22	0	0
		%	0	0	2.75E-22	0	0	0	2.75E-22	0
		%	0	0	0	4.29E-22	0	0	0	4.29E-22
in_alpha = [		%	0	0	0	0	0	0	0	0
		%	0	0	0	0	0	0	0	0
		%	0	0	0	0	0	0	0	0
		%	0	0	0	0	0	0	0	0
in_alpha_p = [		%	0	0	0	0	0	0	0	0
		%	0	0	0	0	0	0	0	0
		%	0	0	0	0	0	0	0	0
		%	0	0	0	0	0	0	0	0
in_eta_i = [		%	0.053	0.191	0.318	0.440	0.053	0.191	0.318	0.440
		%	0.007	0.019	0.027	0.040	0.007	0.019	0.027	0.040
		%	0.007	0.106	0.245	0.291	0.007	0.106	0.245	0.291
		%	0.003	0.046	0.105	0.224	0.003	0.046	0.105	0.224
in_eta_p_i = [		%	0	0	0	0	0	0	0	0
		%	0	0	0	0	0	0	0	0
		%	0	0	0	0	0	0	0	0
		%	0	0	0	0	0	0	0	0
in_eta_e = [		%	1.77E-03	6.46E-05	4.52E-04	3.87E-04	1.77E-03	6.46E-05	4.52E-04	3.87E-04
in_eta_p_e = [		%	0	0	0	0	0	0	0	0
in_eta_ph = [		%	1.50E-04	4.00E-06	1.50E-05	2.50E-05	1.50E-04	4.00E-06	1.50E-05	2.50E-05
in_eta_p_ph = [		%	0	0	0	0	0	0	0	0
in_Cbs = [	[l/s/m]	%	0	0	0	0	0	0	0	0
		%	0	0	0	0	0	0	0	0
		%	0	0	0	0	0	0	0	0
		%	0	0	0	0	0	0	0	0
in_Qth = [		%	1.00E-12	5.00E-15	1.00E-14	5.00E-15	1.00E-12	5.00E-15	1.00E-14	5.00E-15
in_n_e = [		%	0	0	0	0	0	0	0	0
in_N_e = [	[e-/m/s]	%	1.2E+14	0	0	0	1.2E+14	0	0	0
in_Gamma_ph	[ph/m/s]	%	3E+15	0	0	0	3E+15	0	0	0
in_S_Nplus1 =	[l/s] (H2)	%	1147.73	0	0	0	0	0	0	0
	[l/s] (CH4)	%	0	1147.73	0	0	0	0	0	0
	[l/s] (CO)	%	0	0	1147.73	0	0	0	0	0
	[l/s] (CO2)	%	0	0	0	1147.73	0	0	0	0
in_g_Nplus1 =	[torrl/s]	%	0	0	0	0	0	0	0	0

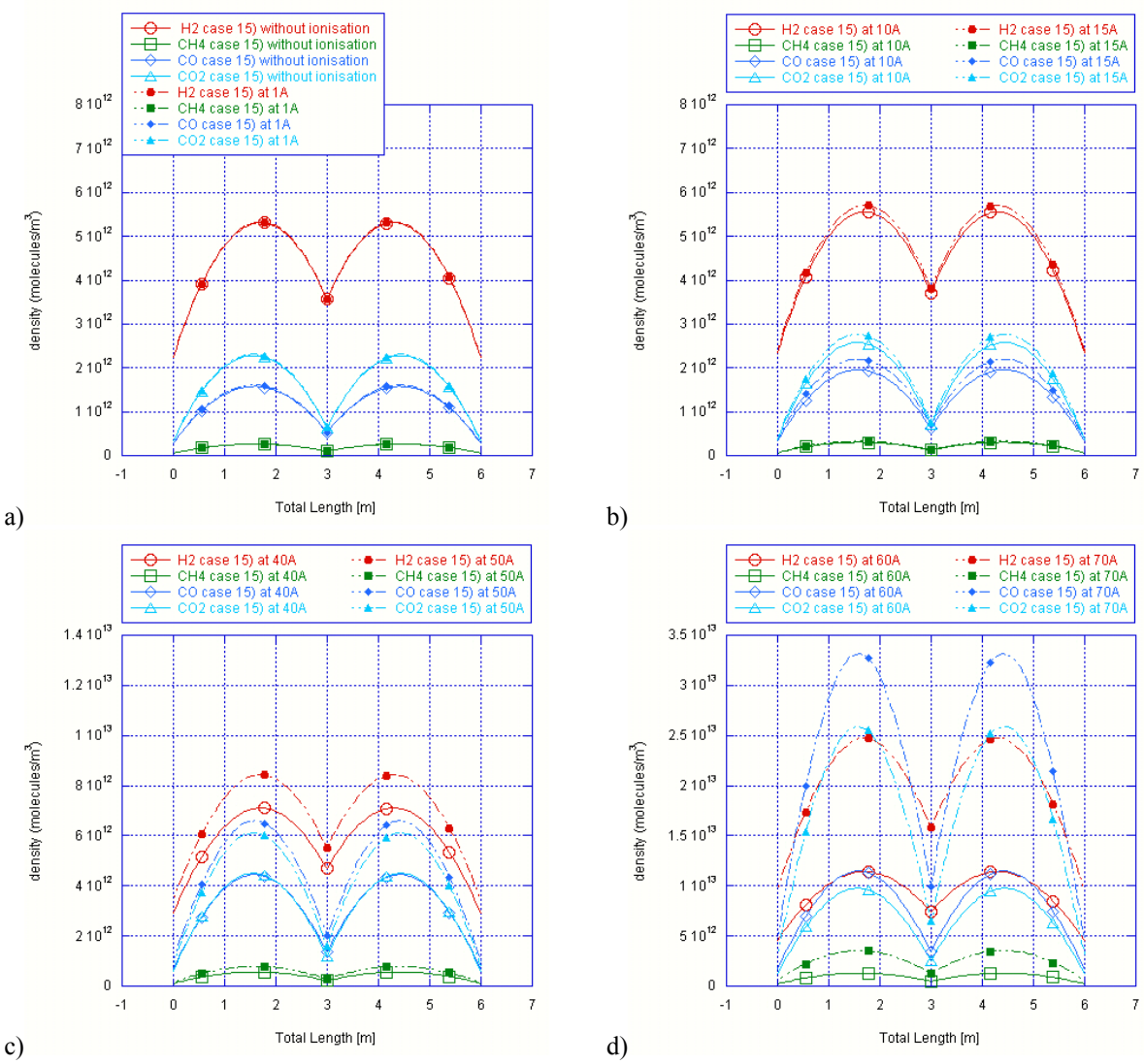

Figure 24 Density profile for Case 15 at a) 0 and 1A beam current; b) 10 and 15A beam current; c) 40 and 50A beam currentt; d) 60 and 70A beam current.

12. Summary

In this paper the VASCO code for critical current and residual gas pressure estimation in a vacuum system has been presented. The VASCO has been conceived for an accelerator with hadron beam operation, but can be easily adapted to other types of vacuum system.

A detailed description of the equation solved by the code, including the methodology used, is given.

The code has been validated, where possible, against a different program used for vacuum calculations, the PRESSURE code. Moreover, VASCO software has been successfully tested against parameter variations.

More importantly, when real cases input parameters are used, the results of VASCO are in agreement with what observed in the ISR when pressure runaway occurred.

Acknowledgments

The author is very greatful to Luigi Scibile for his support at the beginning of the code development. Many thanks to Noel Hilleret and Miguel Jimenez for the fruitful discussion when testing the code.

13. References

[1] A. Mathewson, Maui, Hawaii, November 3-9, 1994.
[2] O.B. Malyshev and A. Rossi, Vacuum Technical Note 99-20, CERN, Geneva 1999.
[3] Code PRESSURE developed by A. Poncet and A. Pace at CERN.
[4] A. Rossi and N. Hilleret, LHC Project Report 674, CERN, Geneva, 18 September 2003.
[5] M.P. Lozano, Vacuum Technical Note 01-05, CERN, Geneva, 2001.
[6] O.B. Malyshev, proc. to EPAC 2000, 26-30 June 2000, Austria Center Vienna.
[7] A.G. Mathewson CERN-ISR-VA 76-05, CERN, Geneva, 1976.
[8] N. Hilleret CERN-ISR-VA 80-17, Geneva, 1980.
[9] R.S. Calder, Vacuum 24, No. 10, 1974, 437-443.